TECHNICAL REPORT BRL-TR-2927

BRL

1938 – Serving the Army for Fifty Years – 1988

COMBINED PRESSURE-SHEAR IGNITION SENSITIVITY TEST

VINCENT M. BOYLE
DEBORAH L. PILARSKI
OLIVER H. BLAKE

JULY 1988

U.S. ARMY LABORATORY COMMAND

BALLISTIC RESEARCH LABORATORY

ABERDEEN PROVING GROUND, MARYLAND

DESTRUCTION NOTICE

Destroy this report when it is no longer needed. DO NOT return it to the originator.

Additional copies of this report may be obtained from the National Technical Information Service, U.S. Department of Commerce, Springfield, VA 22161.

The findings of this report are not to be construed as an official Department of the Army position, unless so designated by other authorized documents.

The use of trade names or manufacturers' names in this report does not constitute indorsement of any commercial product.

REPORT DOCUMENTATION PAGE

Form Approved
OMB No. 0704-0188

1a. REPORT SECURITY CLASSIFICATION UNCLASSIFIED	1b. RESTRICTIVE MARKINGS
2a. SECURITY CLASSIFICATION AUTHORITY	3. DISTRIBUTION/AVAILABILITY OF REPORT Unlimited; approved for public release.
2b. DECLASSIFICATION/DOWNGRADING SCHEDULE	
4. PERFORMING ORGANIZATION REPORT NUMBER(S) BRL-TR-2927	5. MONITORING ORGANIZATION REPORT NUMBER(S)
6a. NAME OF PERFORMING ORGANIZATION USA Ballistic Research Laboratory 6b. OFFICE SYMBOL (If applicable)	7a. NAME OF MONITORING ORGANIZATION
6c. ADDRESS (City, State, and ZIP Code) Aberdeen Proving Ground, MD 21005-5066	7b. ADDRESS (City, State, and ZIP Code)
8a. NAME OF FUNDING/SPONSORING ORGANIZATION 8b. OFFICE SYMBOL (If applicable)	9. PROCUREMENT INSTRUMENT IDENTIFICATION NUMBER
8c. ADDRESS (City, State, and ZIP Code)	10. SOURCE OF FUNDING NUMBERS PROGRAM ELEMENT NO. / PROJECT NO. / TASK NO. / WORK UNIT ACCESSION NO.

11. TITLE (Include Security Classification)
Combined Pressure-Shear Ignition Sensitivity Test

12. PERSONAL AUTHOR(S)
Vincent M. Boyle, Deborah L. Pilarski, Oliver H. Blake

13a. TYPE OF REPORT	13b. TIME COVERED FROM _____ TO _____	14. DATE OF REPORT (Year, Month, Day)	15. PAGE COUNT

16. SUPPLEMENTARY NOTATION

17. COSATI CODES		
FIELD	GROUP	SUB-GROUP

18. SUBJECT TERMS (Continue on reverse if necessary and identify by block number)
Activator; Pressure-Shear Ignition; CMDB Propellant Ignition; TNT Ignition; Comp B Ignition; Shear Band; Viscous Heating

19. ABSTRACT (Continue on reverse if necessary and identify by block number)

A procedure is described for using a high pressure activator to test explosives and propellants for sensitivity to ignition under conditions of combined pressure and shear. Data are presented for TNT and Comp B explosive and CMDB propellant showing that sensitivity increases from TNT to Comp B to CMDB. The maximum pressure and shear velocity were around 1.0 GPa and 60 m/sec, respectively. An analysis of the data in terms of viscous heating of the shear zone is presented. In this analysis, the energy deposition rate per unit volume (due to viscous heating) was equated to the energy loss rate per unit volume (due to thermal conduction) to obtain a relationship between pressure and shear velocity required for ignition. This relationship, $e^{\frac{P}{p}} R V_1^2 = \text{constant}$, defines a boundary curve in the pressure-shear velocity plane between ignition and non-ignition. In this equation, e is the base of the natural logarithm,

20. DISTRIBUTION/AVAILABILITY OF ABSTRACT	21. ABSTRACT SECURITY CLASSIFICATION
☐ UNCLASSIFIED/UNLIMITED ☐ SAME AS RPT ☐ DTIC USERS	UNCLASSIFIED
22a. NAME OF RESPONSIBLE INDIVIDUAL Vincent M. Boyle	22b. TELEPHONE (Include Area Code) (301) 278-6552
22c. OFFICE SYMBOL SLCBR-TB-EE	

DD Form 1473, JUN 86 — Previous editions are obsolete. — SECURITY CLASSIFICATION OF THIS PAGE

BLOCK 19 (Cont)

P is pressure required for ignition, P_R is an experimentally determined constant, and V_1 is shear velocity required for ignition.

*CMDB is an acronym for Composite Modified Double Base.

TABLE OF CONTENTS

FIGURES

FIGURES
(Cont)

TABLES

1. INTRODUCTION

The sensitivity of explosive materials to various stimuli is important both for safe handling as well as functional application. Workers in the energetic materials field have used various tests to categorize explosive sensitivity.[1] Some of the commonly used tests are drop weight impact, small and large scale gap, wedge, bullet impact, and skid tests. These tests cover a wide range of ignition conditions ranging from pressures of hundreds of atmospheres and times of millisecs (skid test) to pressures of 10 GPa and times of microseconds (wedge test). In the explosives community there appears to be general agreement that for shock ignition of heterogeneous explosives, the concentration of shock wave energy at irregularities in the explosive heats a small region of explosive to a temperature high enough that an accelerating chemical reaction ensues. A number of likely energy-concentrating mechanisms have been proposed such as hydrodynamic hot spots, microjet formation at cavities in the explosive, and explosive shear under pressure.[2] Any one or all of these mechanisms may be operative in a shock sensitivity test. Relatively low pressure tests such as the drop weight impact and skid tests exhibit phenomena that suggest a combined pressure-shear mechanism of ignition.[3,4,5]

When we speak of a combined pressure-shear mechanism, we assume that under pressure explosive shear occurs either at local irregularities within the explosive or at boundary discontinuities. This relative motion of adjacent explosive layers under pressure causes frictional/viscous heating of the interlayer. The explosive heats fastest in the region of maximum velocity gradient across the interlayer. Since viscosity decreases as temperature increases, the shear is further localized, i.e., the velocity gradient increases. This localized heated region or shear band would appear to be a likely site for ignition. The experiments reported here have been designed to test the effect of combined pressure-shear on explosive ignition.

2. EXPERIMENTAL DETAILS

In order to test the effect of combined pressure-shear on explosive ignition, we used two different experimental arrangements. One was designed to test explosive sliding against a steel surface, and the other to test explosive shearing and sliding against itself. For brevity, we will refer to these arrangements as explosive on steel and explosive on explosive, respectively.

The first arrangement, explosive on steel, is shown in cross section in Figure 1. A short cylinder of explosive was placed within a steel confinement cylinder. A polyethylene buffer plug was butted against each face of the explosive sample and then the transfer piston and velocity piston were slid into place as shown. The purpose of the polyethylene buffer plugs was to prevent spurious ignition caused by steel on steel friction in the region adjacent to the explosive sample. Dimensions are given in Table 1.

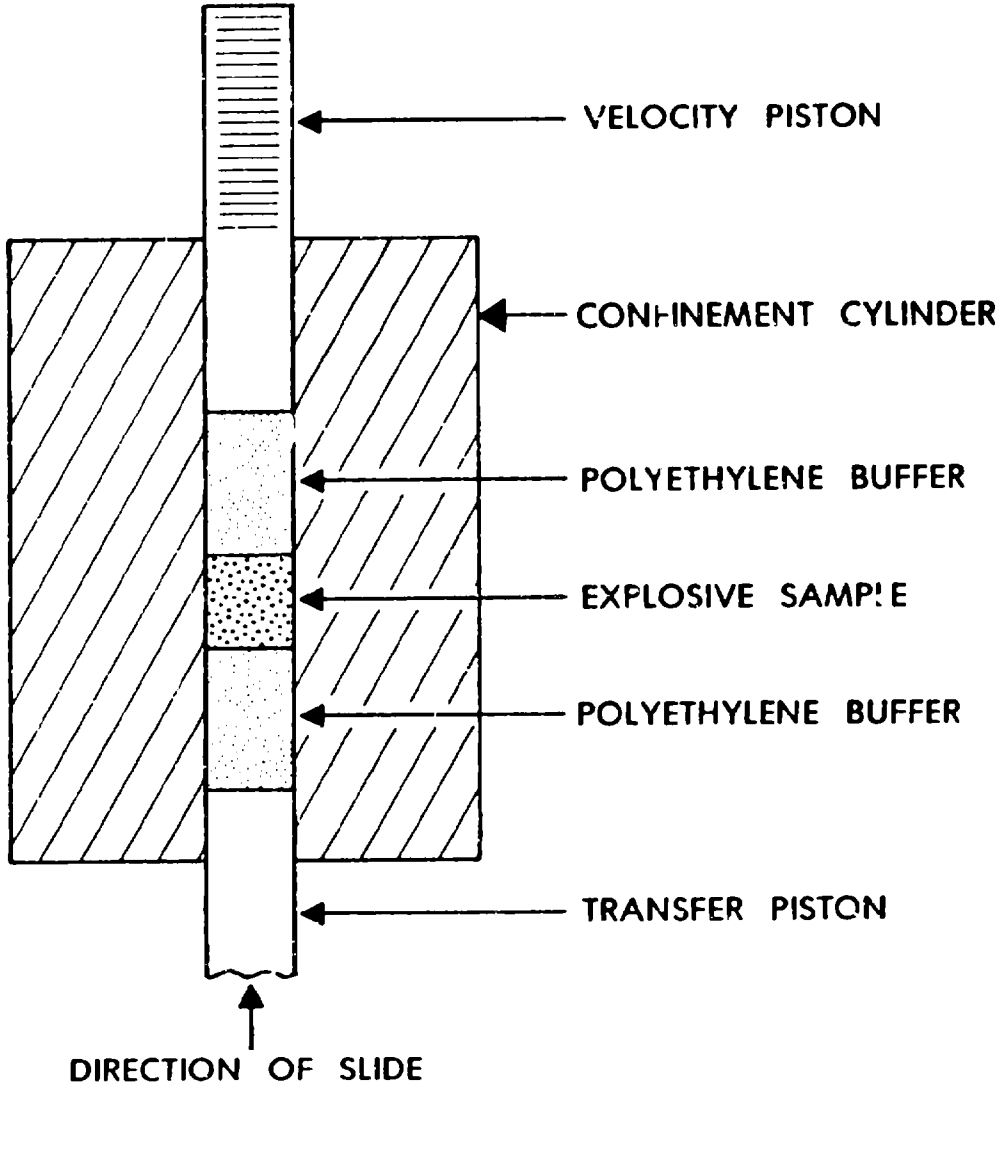

Figure 1. Test Arrangement for Explosive Sliding on Steel

TABLE 1. Test Sample Assembly for Explosive on Steel Shear

Component	Length (mm)	Diameter (mm)	Weight (grams)
Confinement Cylinder	82.6	63.5	
Cylinder Bore	82.6	$12.725^{+.013}_{-0.000}$	
Transfer Piston	69.9	$12.700^{+.013}_{-.013}$	
Velocity Piston	57.2	$12.700^{+.013}_{-.013}$	
Buffer Plugs	19.1	$12.700^{+.025}_{-.025}$	
Explosive Sample	12.7	$12.700^{+.013}_{-.013}$	2.6

2.3 For explosive on explosive shear, we used the arrangement shown in Figure 2. In this case, the explosive sample was clamped within steel sleeves and a plug was sheared out of its center. Dimensions are given in Table 2. Either of these arrangements could be placed in the high pressure activator as shown in Figure 3.

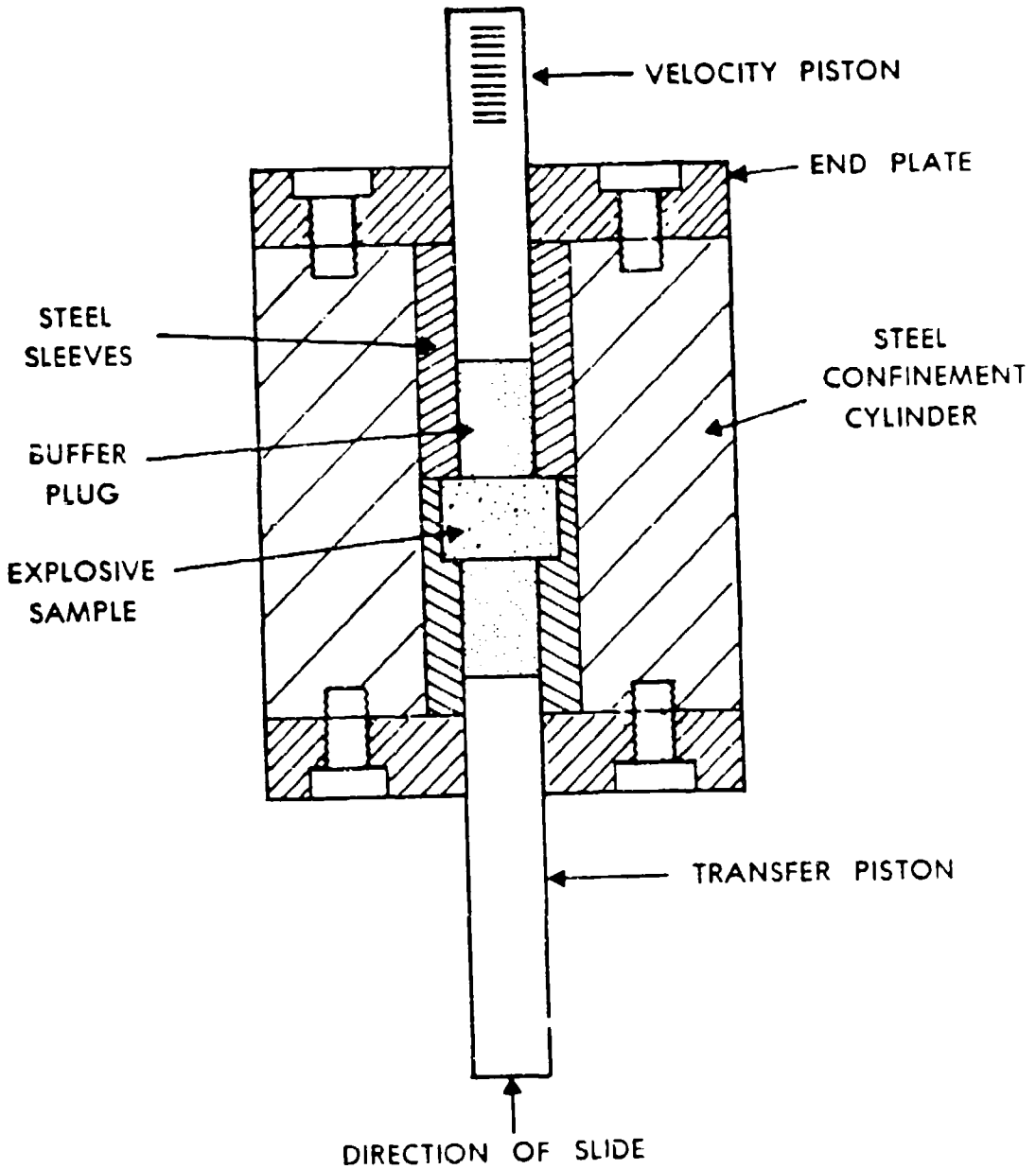

Figure 2. Test Arrangement for Explosive Sliding on Explosive

TABLE 2. Test Sample Assembly for Explosive on Explosive Shear

Component	Length (mm)	Diameter (mm)	Weight (grams)
Confinement Cylinder	76.2	76.2	
Confinement Cylinder Bore	76.2	25.4	
Steel Sleeves	38.1	25.4 (Sliding Fit in Cylinder Bore)	
Steel Sleeve Bore	25.4, 38.1	$12.725^{+.013}_{-0.000}$	
Seat for Test Sample	$12.700^{+.025}_{-0.000}$	$19.075^{+.013}_{-.013}$	
Transfer Piston	69.9	$12.700^{+.013}_{-.013}$	
Velocity Piston	57.2	$12.700^{+.013}_{-.013}$	
Buffer Plugs	19.1	$12.700^{+.025}_{-.025}$	
Test Sample	$12.700^{+.013}_{-.013}$	$19.050^{+.013}_{-.013}$	5.9
End Plates	12.7	76.2	

The end plates were hardened to 40 on the Rockwell C scale and fastened to the confinement cylinder with six 3/8-16 x 3/4 socket head cap screws.

The high pressure activator is a modification of the one described in reference 6. A heavier powder load was used in the breech in order to obtain higher pressures and the breech was continuously vented in order to decrease damage to the activator components. A manganin foil pressure gage was used to measure pressure on the explosive sample and a photodetection system was used to obtain sliding velocity. The activator was used in its contact mode (transfer piston in contact with the breech piston) in order to avoid shock formation which could occur if the breech piston impacted the transfer piston. M-9 propellant was used to pressurize the breech because it left little residue and made clean-up easier. However, it has a high flame temperature and is therefore more erosive to the breech vent hole than a lower flame temperature propellant would be. For this reason, a replaceable nozzle of maraging steel was used as shown in Figure 3.

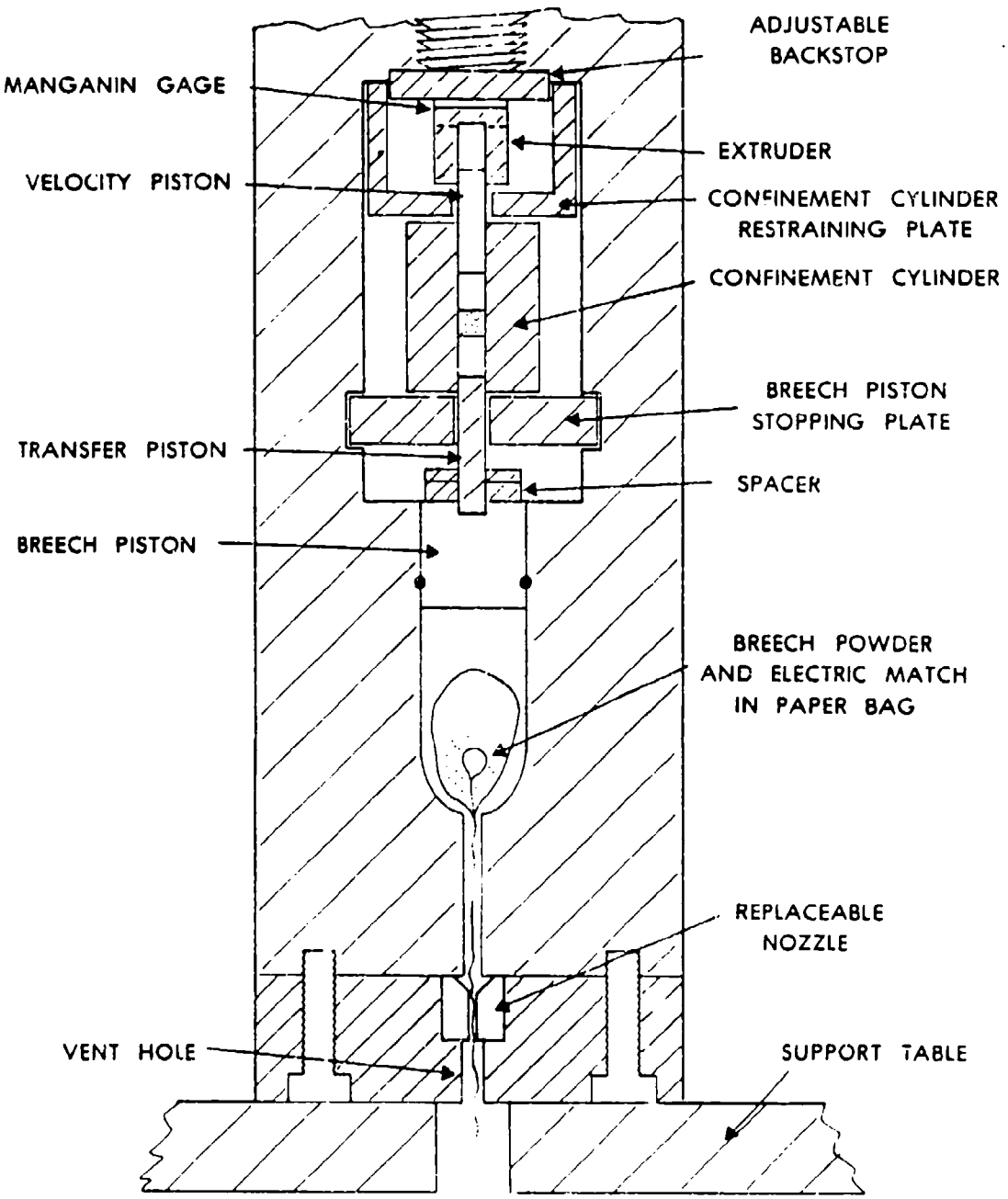

Figure 3. High Pressure Activator

2.1 Test Procedure. For the explosive on steel shear experiments, the explosive test sample was either cast TNT, density = 1.60 gm/cm^3, or cast Comp B, density = 1.69 gm/cm^3. The sample was cast 25.4mm long x 12.7mm diameter and sawed to a length of 12.7mm. The sawed end was sanded using 600 grade emery paper under water. The sample was cleaned and then radiographed for possible voids or flaws. The explosive sample was positioned in the confinement cylinder bore and the polyethylene buffer plugs were inserted as indicated in Figure 1. The purpose of the buffer plugs was to preserve the region of the bore adjacent to the explosive sample free from high temperatures that could be generated by the steel piston rubbing against the bore surface. The bore had a reamed surface finish of 40 micron root mean square. A close-running fit of the sliding parts to the confinement cylinder bore was maintained in order to prevent or minimize extrusion of the explosive or buffer plugs when slid under pressure. Dimensions of the explosive on steel test assembly are shown in Table 1. The confinement cylinder was 1020 mild steel and the pistons were 4340 steel heat treated to 40 on the Rockwell C scale.

2.2 Activator Loading and Assembly. During the course of this investigation, several different loading and assembly procedures were used. The failure element which determines the pressure applied to the explosive sample has undergone several design changes also. Figure 4 represents the current experimental arrangement.

In order to prepare the activator for firing, we weighed M-9 propellant powder and sealed it in tissue paper along with an electric match. This was placed in the breech chamber with the electric match lead wires sticking out of the vent hole. The breech chamber bore was wiped clean and the 50.8mm diameter breech piston was inserted. A 12.7mm thick steel spacer ring (to limit breech piston travel) and a 3.2mm thick polyethylene ring (to cushion piston impact) were placed on the breech piston. A 25.4mm thick hardened steel stopper plate was slid into position 25.4mm above the breech piston. This plate stops the travel of the breech piston.

Next, the transfer piston was positioned in a central indent in the breech piston and the confinement cylinder assembly was slid onto the transfer piston. The restraining plate was placed on the end of the confinement cylinder and tightened against the body of the activator in order to prevent the confinement cylinder from moving due to the frictional force on its bore surface during pressurization. Then the velocity piston, extruder failure element, and manganin foil pressure gage were positioned as shown in Figure 3. Finally, the adjustable backstop was tightened to hold the assembled activator components in place.

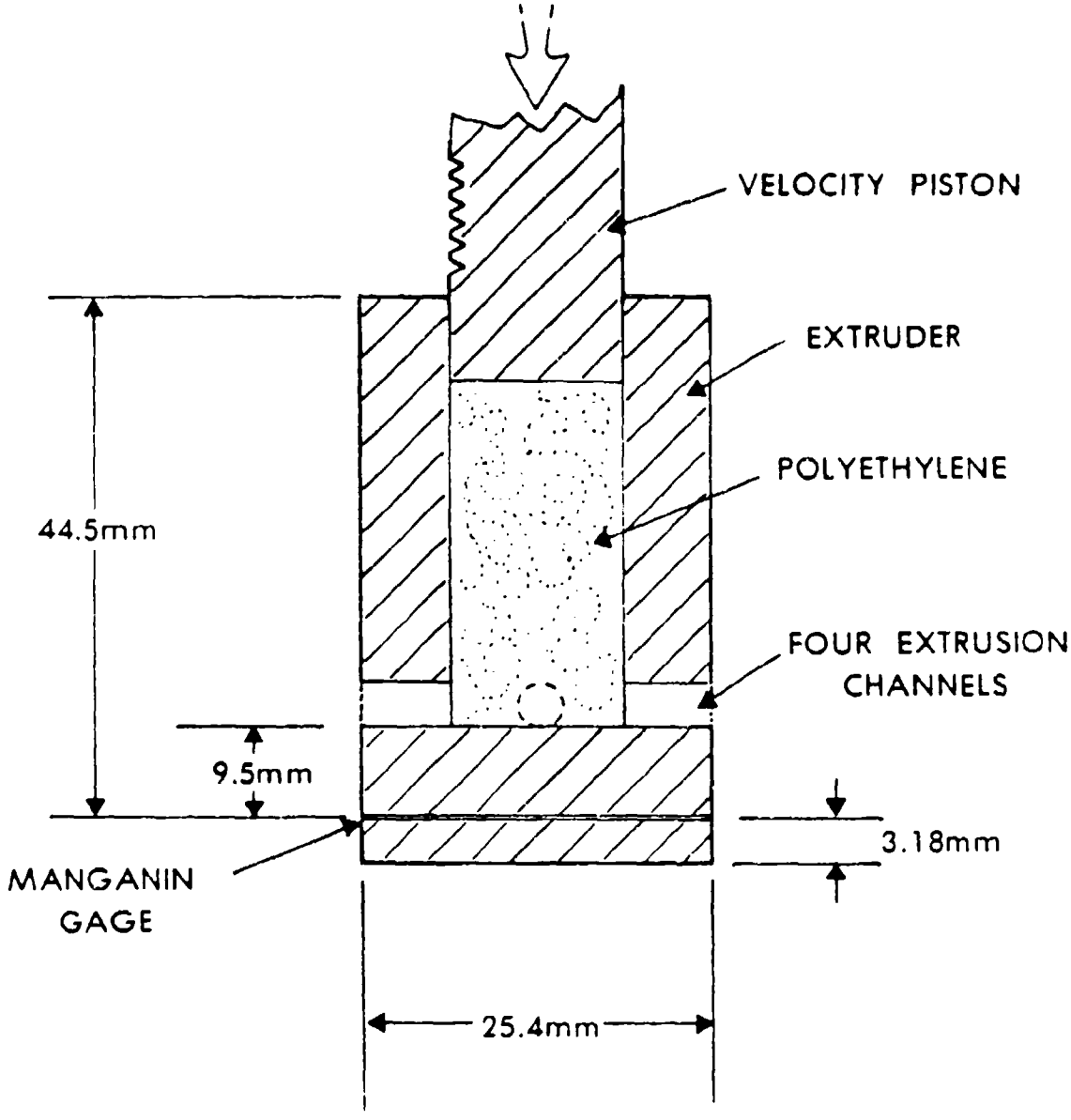

Figure 4. The pressure applied to the explosive sample is determined by the failure element. Polyethylene is extruded through various diameter channels in order to obtain a range of pressures.

2.3 Velocity Measurement. The velocity piston was a standard steel piston which had been modified by machining 0.5mm wide flats separated by 0.5mm wide grooves near one end of the piston as shown in Figure 5. These flats were polished to a final finish using .01 micron aluminum oxide powder. In order to measure the sliding velocity of the explosive sample, a one milliwatt helium-neon laser beam was reflected from the velocity piston through an interference filter and into a 1P22 photomultiplier tube. The motion of the piston was measured by feeding the phototube output signal to a Data Precision Model 6000 waveform analyzer. As each reflecting flat on the velocity piston intercepted the laser beam, a voltage signal was generated. Knowing the distance between flats (1mm center to center) and measuring the time between voltage peaks, we were able to calculate the sliding velocity.

2.4 Pressure Measurement. The pressure on the explosive sample was measured by using a piezoresistive manganin foil pressure gage sandwiched between two steel surfaces downstream from the explosive sample as shown in Figure 3. Since the activator is used in the contact mode, the pressure pulse measured at this point is probably a good representation of the pressure pulse on the explosive sample. However, due to frictional force along the confinement cylinder bore, the downstream region may experience a somewhat lower pressure than the sample region.

The piezoresistive manganin foil gage is sensitive to gage distortion. Great care must be taken to support the gage on a flat surface and to stress the gage and its support uniformly. In our current arrangement (shown in Figure 6) the manganin gage is epoxied between two thin Mylar sheets and this sandwich is epoxied between the ground surfaces of the pressure extruder and a 25.4mm diameter steel plate.

In order to obtain a range of pressures, we extruded polyethylene through various diameter orifices as shown in Figure 6. The extruder body was 4340 steel hardened to 45 on the Rockwell C scale. The base of the extruder was ground flat. There were four holes drilled through the wall of the extruder as shown. The static yield pressure of the polyethylene-filled extruder for various diameter holes was determined experimentally using a Carver laboratory press, Model C. These pressures are indicated in Figure 6. The dynamic yield pressure was generally 20% to 50% higher.

The manganin gage forms one arm of a balanced Wheatstone bridge circuit as shown in Figure 7. When the gage is pressurized, its resistance changes, unbalancing the circuit and producing a voltage output, V, proportional to the pressure, P:

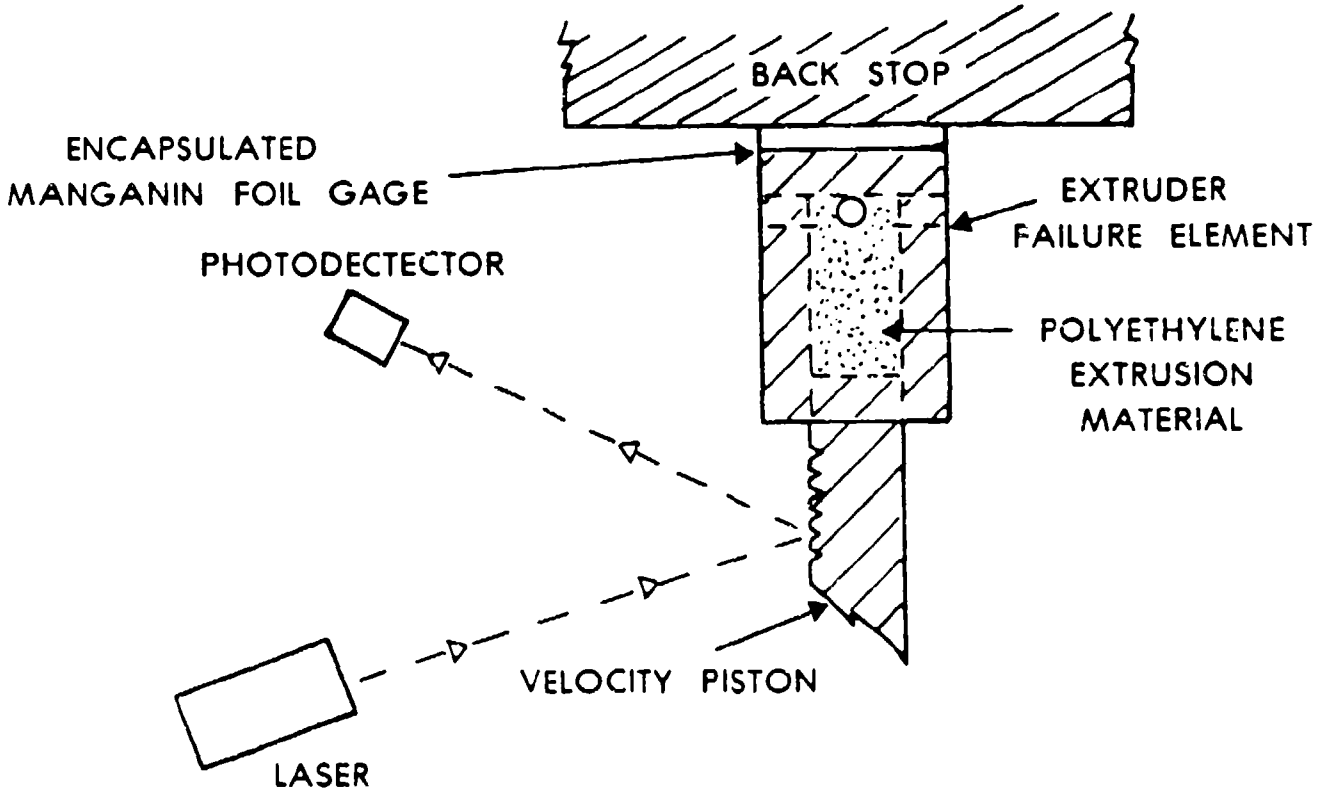

Figure 5. Sliding velocity was calculated by recording the time between laser reflections from flat surfaces spaced one mm apart, center to center.

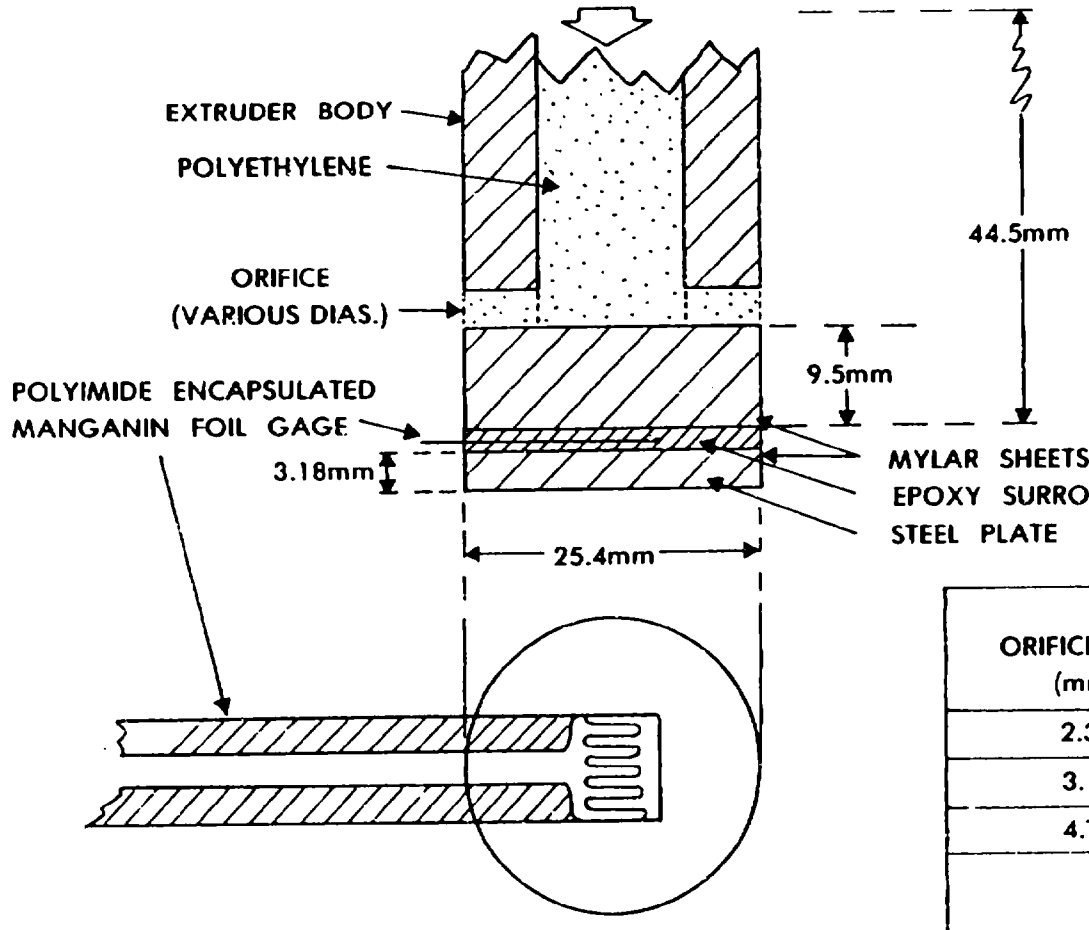

ORIFICE DIA (mm)	STATIC YIELD PRESSURE (GPA)
2.38	.35
3.18	.28
4.76	.11

Figure 6. The manganin gage sandwich was placed between two flat steel surfaces as shown. The static yield pressure of the polyethylene-filled extruder is tabulated for various orifice diameters.

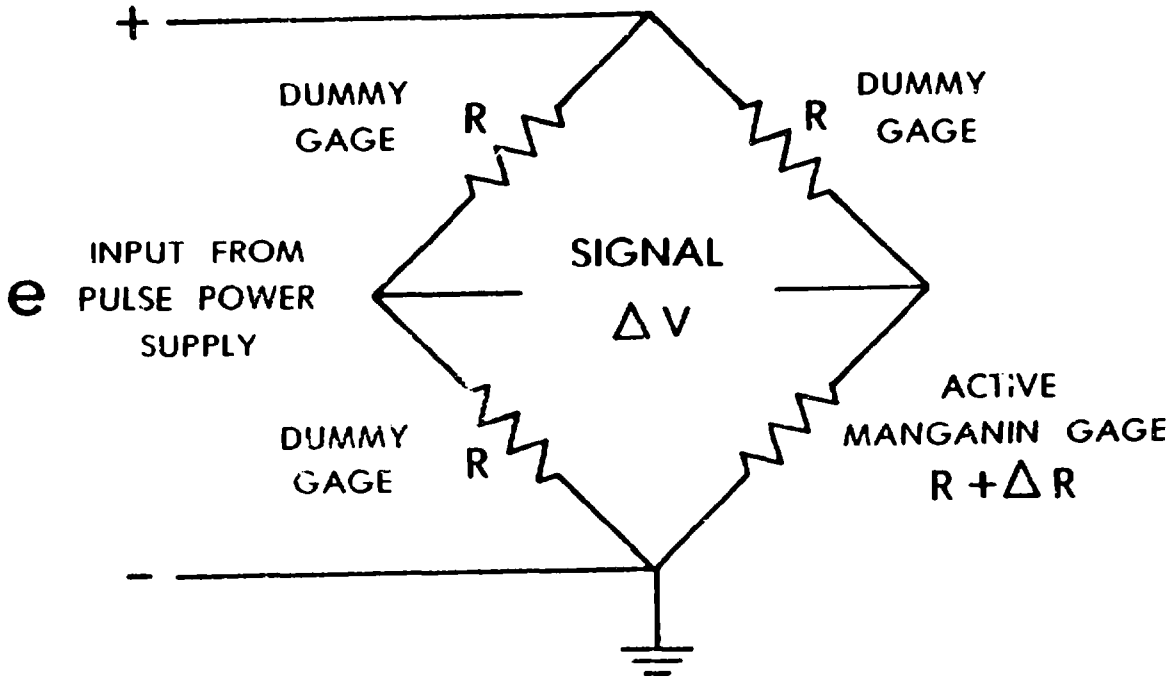

Figure 7. Location of Manganin Gage in a Wheatstone Bridge Circuit

$$P = \frac{4\ \Delta V}{\alpha(e)}$$

where P = Pressure (GPa)
ΔV = Output Signal (Volts)
e = Bridge Input Voltage (Volts)
α = Pressure Coefficient of Resistance for Manganin - $\frac{.023\ \text{ohm}}{\text{ohm - GPa}}$

The derivation of this equation is shown in Appendix A. This is the pressure on the 25.4mm diameter steel plate. In order to calculate the pressure on the 12.7mm diameter explosive sample, we multiplied the measured pressure by $\left(\frac{25.4}{12.7}\right)^2$. This gave a sample pressure four times greater than the measured pressure assuming no frictional losses.

3. RESULTS

Typical pressure and shear displacement records are shown in Figures 8 to 10. Figure 8A illustrates the results obtained for TNT slid against itself without reaction. The upper trace represents the pressure sensed by the manganin foil gage and the lower trace represents the displacement of the velocity piston; the horizontal time axis is 2.048 msecs long. The vertical axis is located at the point of maximum deflection of the upper trace; the pressure on the TNT sample was calculated as explained previously. The average shear velocity occurring at this time is calculated by dividing the distance between the reflecting flats on the velocity piston (1mm) by the time between adjacent peaks on the displacement trace. The data from these records indicate that TNT did not react when slid against itself at a pressure of 0.56 GPa and a velocity of 20 m/sec. As with most of our shots, the maximum pressure was reached within one millisecond.

Figure 8B represents TNT on TNT shear in which reaction occurred. The vertical axis is positioned at the estimated point where reaction occurred. This corresponds to a pressure of 1.08 GPa and a shear velocity of 33.3 m/sec. It can be seen that there is an increase in pressure and piston velocity at this point. There is an increase in pressure and piston velocity at an earlier time but we attribute that to non-uniformities in the pressurization rate due, perhaps, to uneven burning of breech propellant or binding and subsequent releasing of pistons. We have obtained records showing increases in pressure and velocity where reaction did not occur. This figure illustrates the difficulty of picking a precise reaction point.

Figure 9A represents a non-reaction record when Comp B is slid on Comp B at a maximum pressure of 0.92 GPa and a shear velocity of 12.5 m/sec. Figure 9B shows Comp B reacting at a pressure of 1.07 GPa and a shear velocity of 26.3 m/sec. The reaction caused the piston velocity to increase to 100 m/sec within 50 microseconds. The pressure gage recorded 3.1 GPa before it broke.

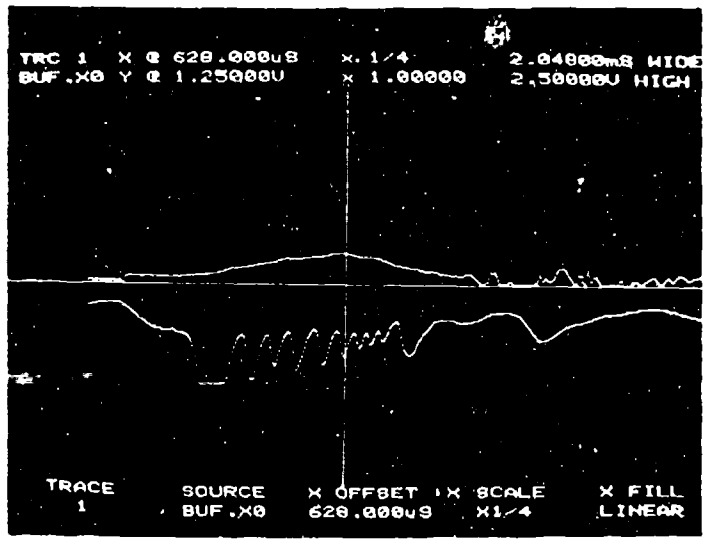

Figure 8A. TNT slid against TNT. No reaction. Upper trace shows manganin foil pressure gage signal. Lower trace shows velocity piston displacement record from which sliding velocity is calculated.

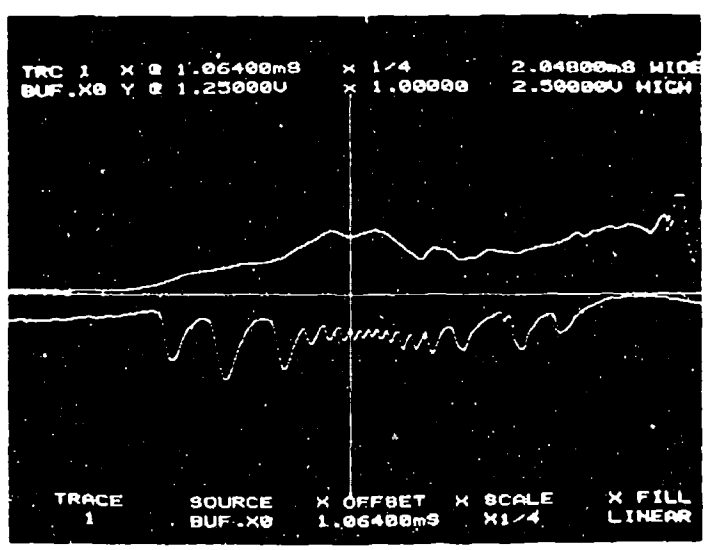

Figure 8B. TNT Slid Against TNT - Reaction

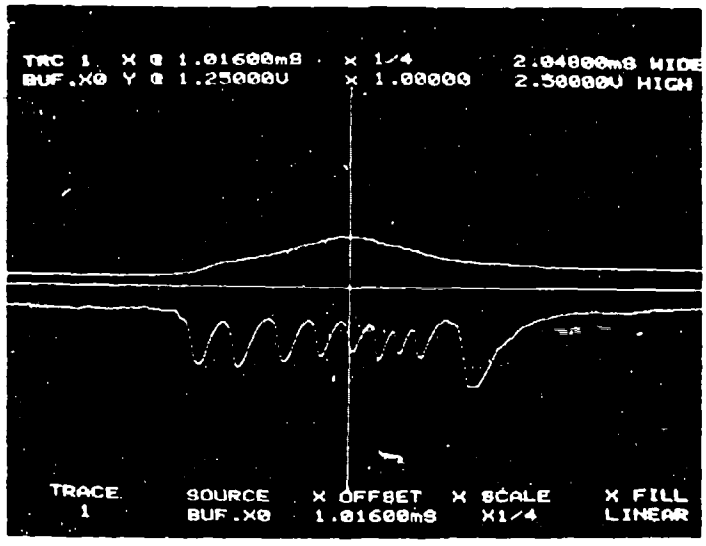

Figure 9A. Comp B Slid Against Comp B - No Reaction

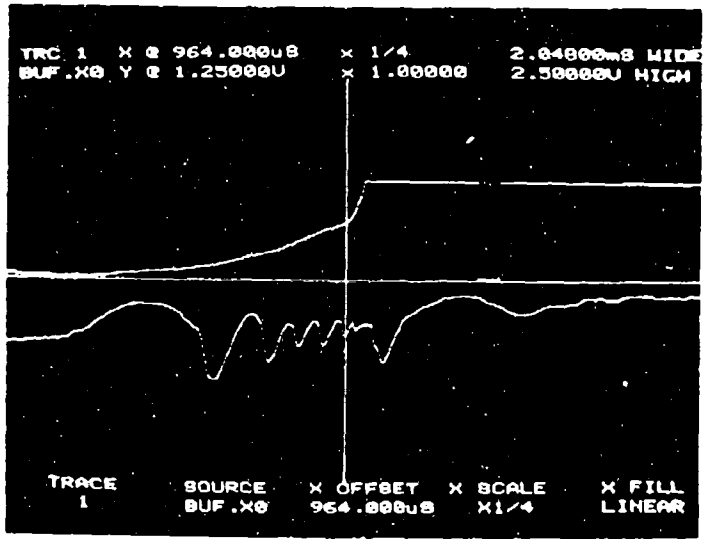

Figure 9B. Comp B Slid Against Comp B - Reaction

Figure 10A shows a non-reaction record when CMDB propellant* is slid upon itself at a pressure of 0.18 GPa and a shear velocity of 17.9 m/sec.

Figure 10B illustrates reaction when CMDB is slid on CMDB. The vertical axis is located at the estimated reaction point. The pressure at this point is 0.25 GPa and the shear velocity is 47.6 m/sec. The pressure drops slightly because the activator breech piston is contacting the stopper plate around this time. Due to reaction, however, the pressure remains high and the piston velocity increases to 80 m/sec. The big jump in the pressure trace is due to the velocity piston impacting the base of the extruder after the material has been extruded.

We have measured the pressure and shear velocity for TNT and Comp B sliding against a steel surface in the configuration illustrated in Figure 1. We have also measured pressure and shear velocity for TNT, Comp B, and FKM propellant slid against themselves as illustrated in Figure 2.

The data for TNT on steel are plotted in Figure 11 as sliding velocity vs peak pressure on the explosive sample. On most shots, the peak pressure and maximum velocity were nearly simultaneous.

The clear and filled symbols represent non-reaction and reaction, respectively. There is wide scatter in the data, some of which may be attributable to experimental problems. However, some of the pressures and velocities may have been increased due to explosive reaction.

The data for Comp B on steel are shown in Figure 12. The data indicate that Comp B is more sensitive than TNT to shear ignition. Also, it is more evident here that there is an inverse relationship between the pressure and velocity required for ignition. The derivation of the solid line superimposed on the data will be explained in the analysis section. It can be loosely interpreted as an isotherm defining the boundary between reaction and non-reaction.

The results for TNT slid on TNT are shown in Figure 13. The critical (isotherm) curve for TNT on steel has been superimposed on these results also. The same isotherm curve has been used for both sets of data.

The results for Comp B slid on Comp B are shown in Figure 14 with the Comp B on steel isotherm curve superimposed.

Finally, the results of CMDB slid on CMDB are presented in Figure 15. The superimposed isotherm for CMDB was calculated as shown in the analysis section. It can be seen that CMDB propellant is much more sensitive to combined pressure-shear ignition than either TNT or Comp B.

*The work on CMDB propellant was funded by the HARP program, NSWC, White Oak, Silver Spring, MD. CMDB is an acronym for Composite Modified Double Base.

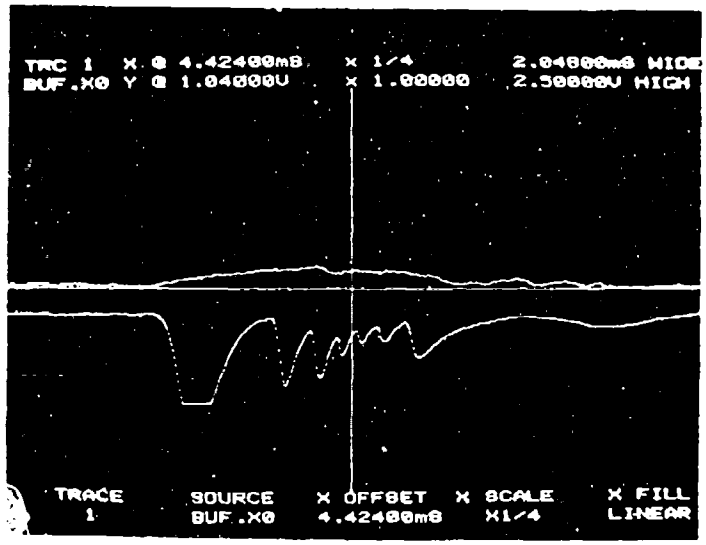

Figure 10A. CMDB Slid Against CMDB- No Reaction

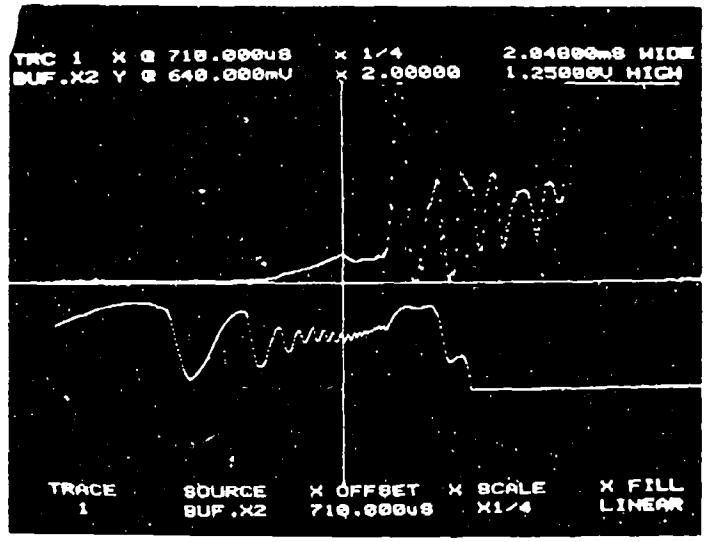

Figure 10B. CMDB Slid Against CMDB - Reaction

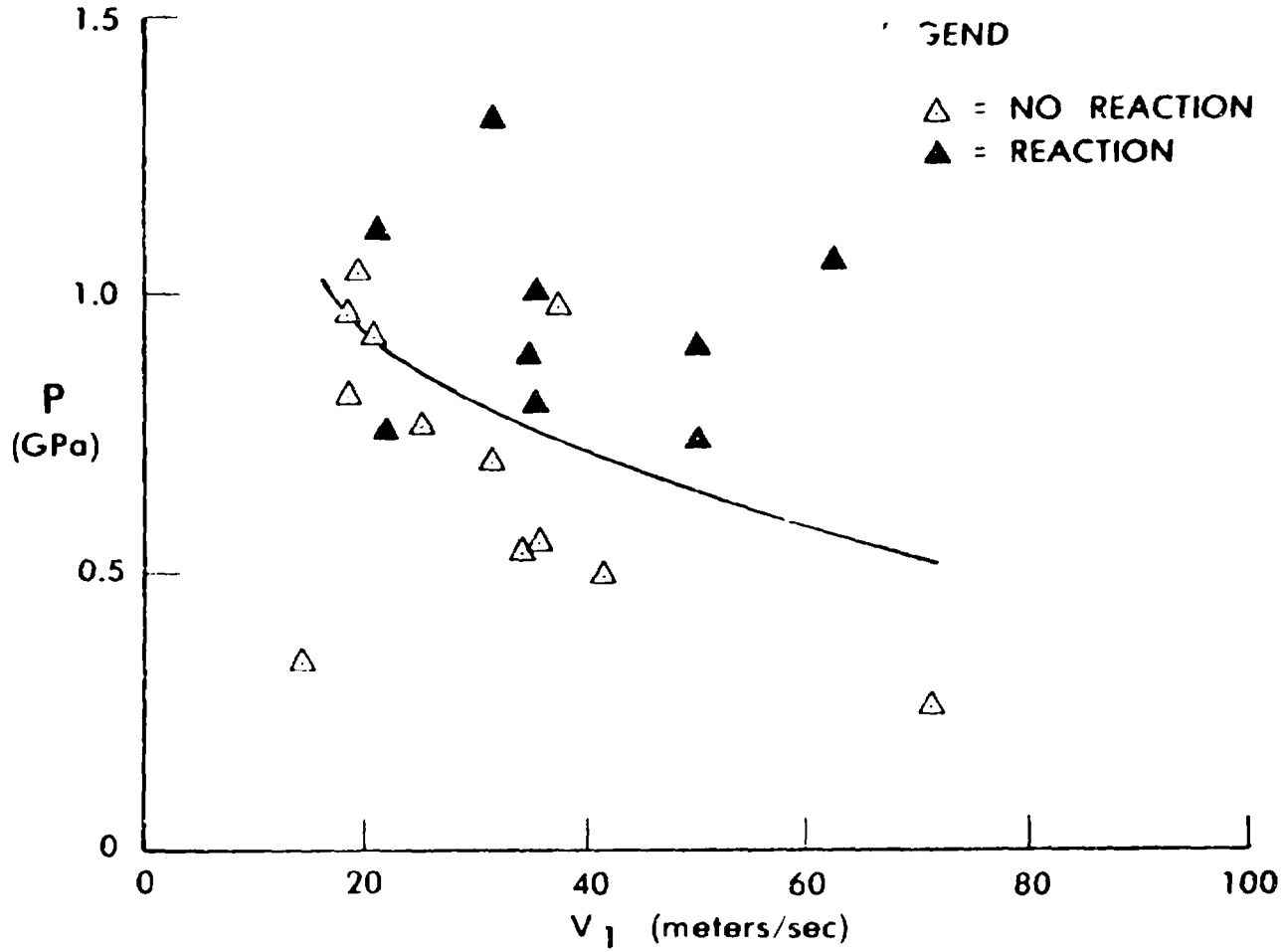

Figure 11. Data for TNT slid against steel showing peak pressure vs sliding velocity where TNT did not react (clear symbols) and estimated pressure vs sliding velocity where TNT reacted (filled symbols). The solid curve represents the boundary between reaction and non-reaction.

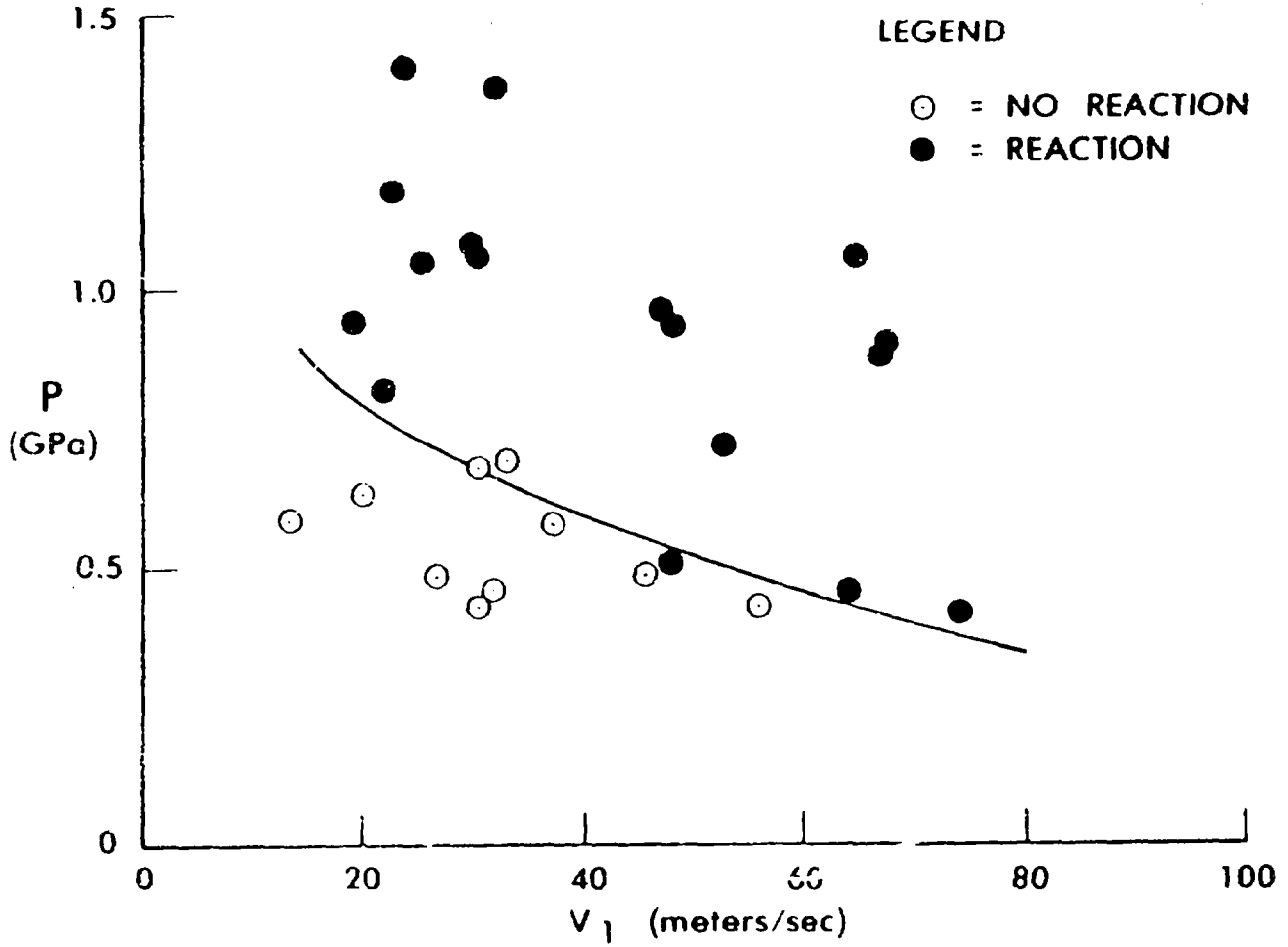

Figure 12. Data for Comp B slid against steel. The solid curve represents the boundary between reaction and non-reaction.

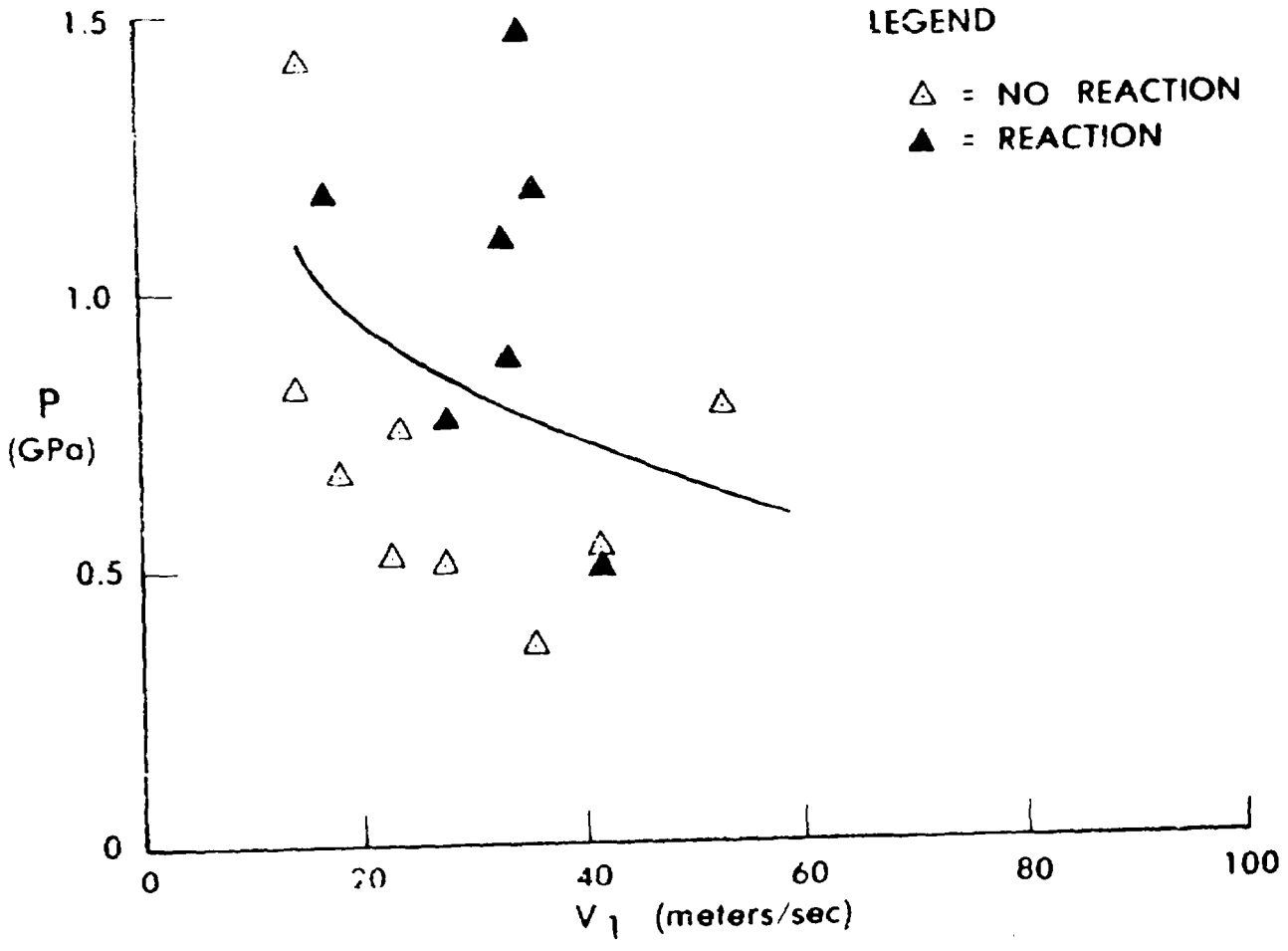

Figure 13. Data for TNT slid against TNT. The solid curve represents the boundary between reaction and non-reaction.

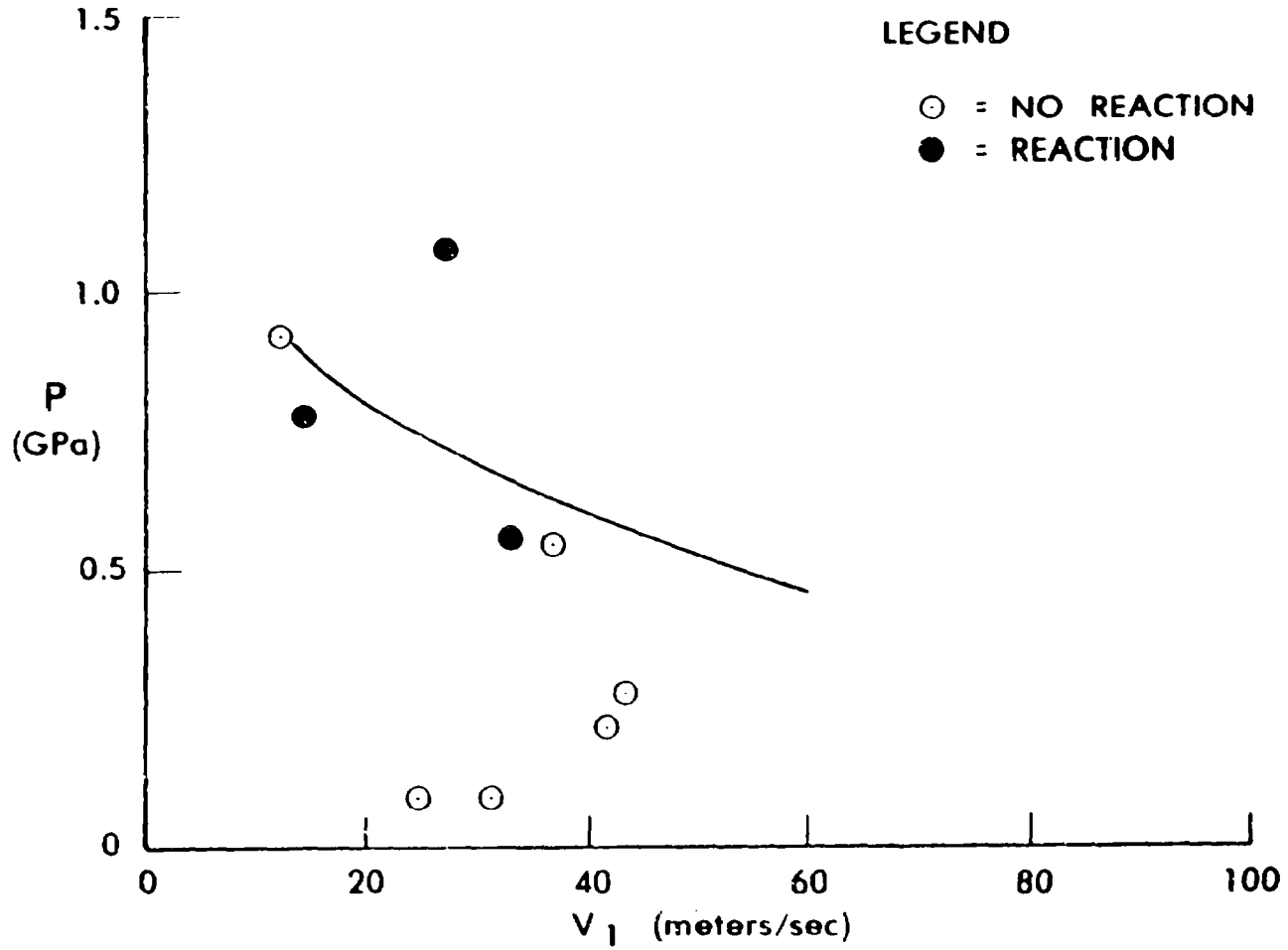

Figure 14. Data for Comp B slid against Comp B. The solid curve represents the boundary between reaction and non-reaction.

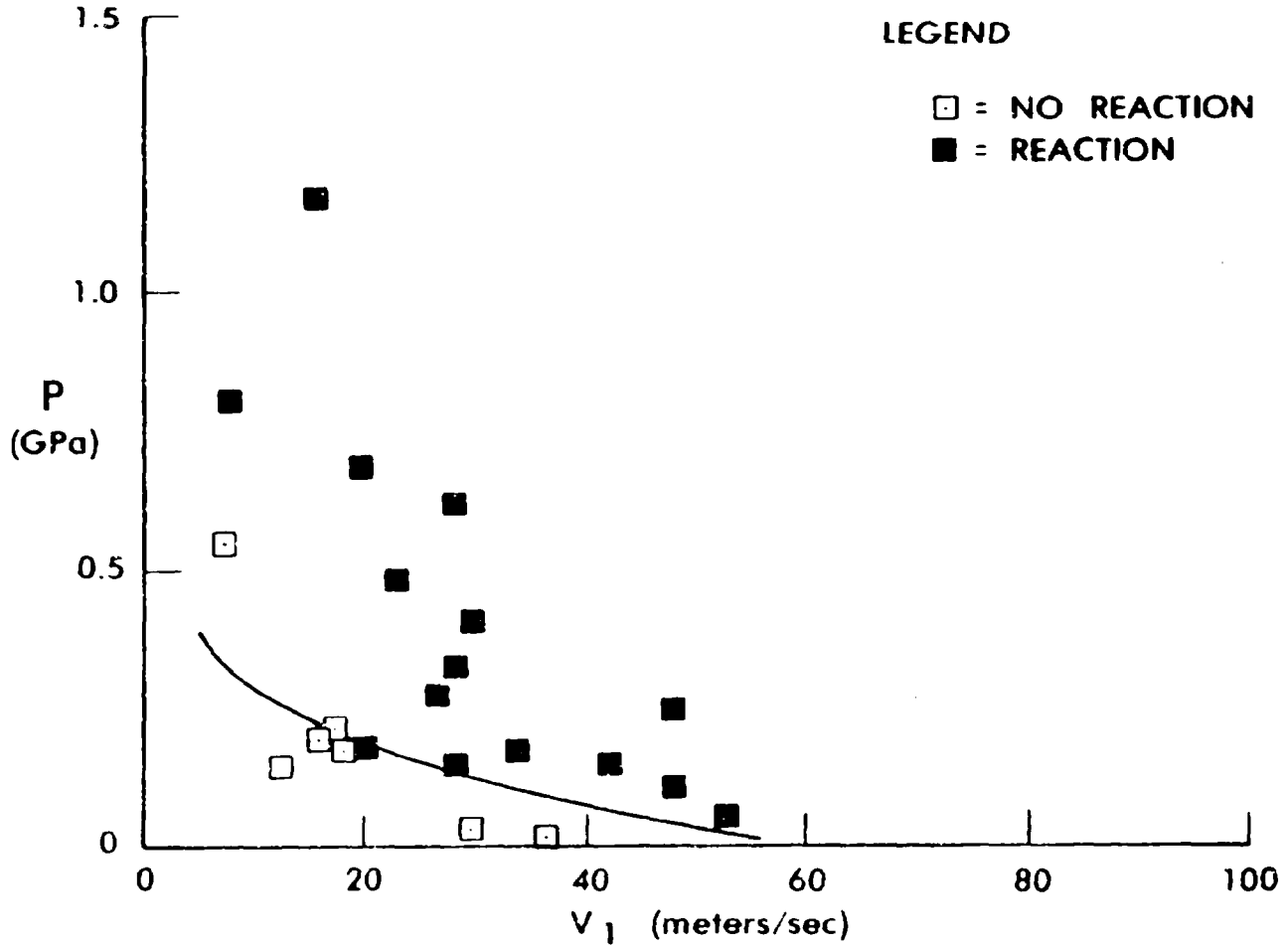

Figure 15. Data for CMDB slid against CMDB The solid curve represents the boundary between reaction and non-reaction.

4. ANALYSIS

We have attempted to correlate our pressure-shear ignition data in terms of viscoplastic heating of the narrow zone of shearing explosive which we will refer to as the shear band. We imagine that as the explosive shears under pressure, thermal energy is deposited in the shear band by viscous heating. The shear band continues to increase in temperature with the highest temperature becoming localized at the center of the shear band due to thermal flow from its boundary. The high temperature at the center decreases the viscosity of the explosive thereby increasing the shear rate in this region. The net result of this viscous heating process is to create a narrow band of heated explosive with the maximum temperature at the center.

The temperature at the center of the shear band will continue to increase until the energy deposition rate per unit volume (due to viscous heating) is balanced by the energy flow rate per unit volume (due to thermal conduction). As the thermal gradient steepens, the energy loss rate per unit volume increases. If the peak temperature is high enough, the explosive will react.

We will heuristically derive a relation between the shear velocity and the pressure at the boundary between reaction and no reaction. Frey7 has treated shear band growth in a more complete fashion, and the relationship which we heuristically derive here has been verified in his model. Figure 16 is an idealization of the temperature and velocity variation across the shear band when peak temperature is reached. The slopes of the dashed lines represent the average values of the temperature and velocity gradient. We will use these average values to relate the thermal energy deposition rate per unit volume to the thermal energy loss rate per unit volume in order to derive a relationship between pressure and shear velocity at the boundary between reaction and non-reaction. Some assumptions made are:

Explosive shear strength is negligible (only viscous forces are important for explosive heating). For Comp B and TNT, this is probably a good assumption because these explosives melt before they react. The maximum temperature occurs in the melt layer. For CMDB, it may be suspect.

Viscosity varies with pressure and temperature as indicated below.

Coefficient of thermal conductivity remains constant.

As mentioned, we used average values of variables across the shear band. These values are listed here and shown in Figure 16.

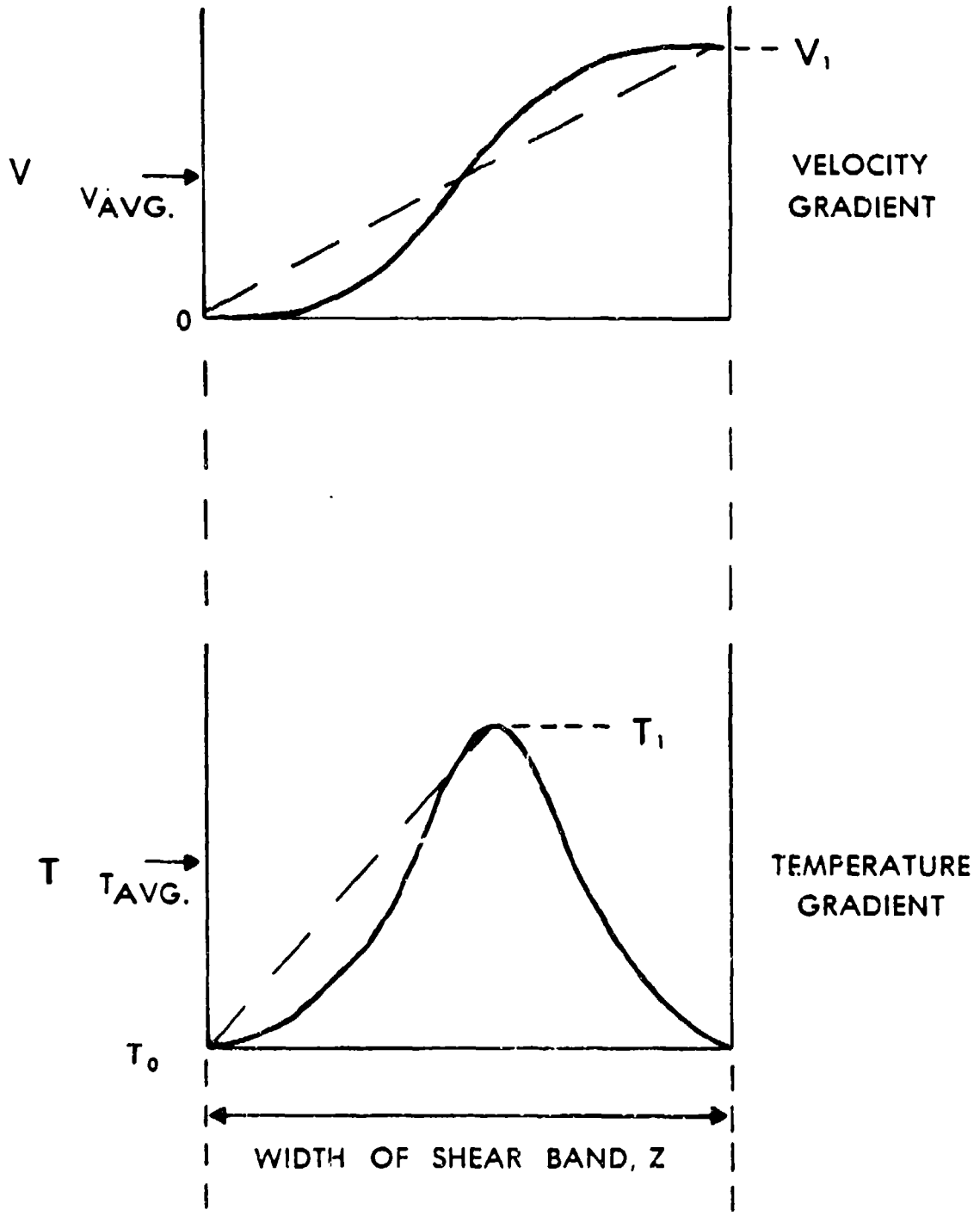

Figure 16. Idealization of the shear velocity and temperature variation across the shear band at the time peak temperature is reached.

$$T_{AVG} = \frac{T_0 + T_1}{2} \qquad \text{(temperature)}$$

$$\frac{\Delta T}{\Delta Z} = \frac{T_1 - T_0}{\frac{Z}{2}} \qquad \text{(temperature gradient)}$$

$$V_{AVG} = \frac{\Delta X}{2\Delta t} = \frac{V_1}{2} \qquad \text{(shear velocity)}$$

$$\frac{\Delta V}{\Delta Z} = \frac{V_1 - 0}{Z} \qquad \text{(shear velocity gradient)}$$

The thermal energy deposition rate per unit volume for a viscous medium under shear can be written as

$$\frac{1}{2}\mu\left(\frac{dV}{dz}\right)^2 \qquad (1)$$

or, using average values,

$$\frac{1}{2}\bar{\mu}\left(\frac{\Delta V}{\Delta Z}\right)^2 \qquad (2)$$

The viscosity, $\bar{\mu}$, increases as pressure increases and decreases as temperature increases. R. Frey[7,8] fit a limited range of data to obtain a relationship for variation of viscosity of molten TNT with temperature. We have used the same relationship. For the viscosity variation with pressure, Frey used a relationship typical of organic liquids such as nitrobenzene. Combining the temperature and pressure corrections, the viscosity dependence of TNT on temperature and pressure can be written as

$$\bar{\mu} = \mu_R e^{\frac{P}{P_R}\left(\frac{E}{T_{AVG}} - \frac{E}{T_R}\right)} \qquad (3)$$

where μ_R = viscosity of TNT at 358°K = 1.39×10^{-2} $\frac{kg}{m\text{-}sec}$ (ref 9,

P = pressure in the shear band, GPa

P_R = experimentally determined constant = 0.165 GPa

E = experimentally determined constant = 3880°K

T_{AVG} = average temperature in the shear band, °K

T_R = 358°K

e = base of the natural log = 2.71828

The average thermal energy deposition rate per unit volume can now be written as

$$1/2\,\mu_R e^{\frac{P}{P_R}\left(\frac{E}{T_{AVG}} - \frac{E}{T_R}\right)} \left(\frac{\Delta V}{\Delta Z}\right)^2 \qquad (4)$$

The thermal energy loss rate per unit volume can be expressed as

$$\lambda_o \left(\frac{\Delta T}{\Delta Z}\right) \frac{1}{Z} \qquad (5)$$

where λ_o = thermal conductivity of TNT at 293°K = $\frac{0.262 \text{ joule}}{\text{m-°K-sec}}$.[9] The thermal conductivity increases relatively slowly with pressure and decreases with temperature. We have treated it as a constant.

As an explosive shears under pressure, energy is concentrated near the center of the shear band by viscous heating while energy is dissipated by thermal conduction across the shear band. If a critical temperature is reached, the explosive will react. Otherwise the explosive will remain unreacted. In our pressure-shear experiments, the boundary between reaction and non-reaction is roughly equivalent to a critical temperature or isotherm. At this critical temperature the energy deposition rate per unit volume is equal to the energy loss rate per unit volume. The curve in Figure 11 is a fit to our pressure-shear data for TNT on steel obtained by equating Equations 4 and 5 as follows:

$$1/2\mu_R e^{\frac{P}{P_R}\left(\frac{3880^\circ}{T_{AVG}} - \frac{3880^\circ}{T_R}\right)} \left(\frac{\Delta V}{\Delta Z}\right)^2 = \lambda_o \left(\frac{\Delta T}{\Delta Z}\right) \frac{1}{Z} \qquad (6)$$

Referring to Figure 16, this can be rewritten as

$$1/2\mu_R e^{\frac{P}{P_R}\left(\frac{3880^\circ}{T_{AVG}} - \frac{3880^\circ}{T_R}\right)} \left(\frac{V_1}{Z}\right)^2 = \lambda_o \left(\frac{T_1 - T_0}{\frac{Z}{2}}\right) \frac{1}{Z}$$

or

$$e^{\frac{P}{P_R}} V_1^2 = \frac{4\lambda_o (T_1 - T_0)}{\mu_R e^{\left(\frac{3880^\circ}{T_{AVG}} - \frac{3880^\circ}{T_R}\right)}} \qquad (7)$$

Note that the shear band width, Z, drops out of the equation. The shear band width varies with time, but it does not affect the maximum temperature in the band. Frey's calculations[7], which relax some of the assumptions used here, also show that the maximum temperature is independent of shear band width.

If we assume that reaction occurs when a critical temperature, T_1, is reached, then, for a given explosive

$$e^{\frac{P}{P_R}} V_1^2 = \text{constant.} \qquad (8)$$

Values for P and V_1 were substituted into Equation 8 until we obtained a curve which seemed to give a good eye fit to the data. The point P = 0.8 GPa, V_1 = 30 m/sec lies on this curve. Using these values and P_R = 0.165 GPa for TNT on steel

$$e^{\frac{P}{P_R}} V_1^2 = e^{\frac{0.800}{0.165}} (30)^2 = 1.15\text{x}10^5 \frac{m^2}{sec^2} \qquad (9)$$

We superimposed the curve defined by Equation 9 on the data for TNT on TNT shear as shown in Figure 13. Although there is a lot of scatter in the two sets of data (TNT on steel and TNT on TNT), Equation 9 gave an adequate fit for both sets.

We proceeded in a similar manner for shear ignition of Comp B on steel. We continued to use P_o = 0.165 GPa since we did not have viscosity data for Comp B. For Comp B on steel

$$e^{\frac{P}{P_R}} V_1^2 = e^{\frac{0.670}{0.165}} (30)^2 = 0.52\text{x}10^5 \frac{m^2}{sec^2} \qquad (10)$$

The lower value of $e^{\frac{P}{P_R}} V_1^2$ for Comp B is a measure of its greater shear ignition sensitivity relative to TNT. This curve is shown in Figure 12 for Comp B on steel data. We superimposed the curve defined by Equation 10 on the data for Comp B on Comp B shear. We had only a small amount of data for this case but the fit seems adequate. This is shown in Figure 14.

For CMDB propellant we did not have any viscosity data, so we assumed that $e^{\frac{P}{P_R}V_1^2}$ = constant, substituted estimated pressure and velocity values at two different points and obtained P_R = .076 GPa for CMDB. propellant. Then, for CMDB on CMDB shear

$$e^{\frac{P}{P_R}V_1^2} = e^{\frac{.117}{.076}(30)^2} = .042\times10^5 \frac{m^2}{sec^2} \qquad (11)$$

Again, the low value of $e^{\frac{P}{P_R}V_1^2}$ relative to TNT and Comp B is an indication of the greater shear sensitivity of CMDB propellant. This curve is shown superimposed on the data in Figure 15.

Figure 17 is an extrapolation of the curves for TNT, Comp B, and CMDB in order to illustrate their relative sensitivities for pressure-shear ignition over a wider range of pressure and shear velocity.

5. SHEAR BAND TEMPERATURE

We can rearrange Equation 7 to indicate the relationship between peak temperature T_1 and various experimental parameters associated with the shear band.

$$\frac{T_1 - T_0}{e^{\frac{3880}{T_{AVG}}}} = \frac{\mu_R e^{\frac{P}{P_R}V_1^2}}{4\lambda_o e^{\frac{3880}{T_R}}} \qquad (12)$$

Since $T_{AVG} = \frac{T_1 + T_0}{2}$, we can write

$$\frac{T_1 - T_0}{e^{\frac{7760}{T_1+T_0}}} = \frac{\mu_R e^{\frac{P}{P_R}V_1^2}}{4\lambda_o e^{\frac{3880}{T_R}}} \qquad (13)$$

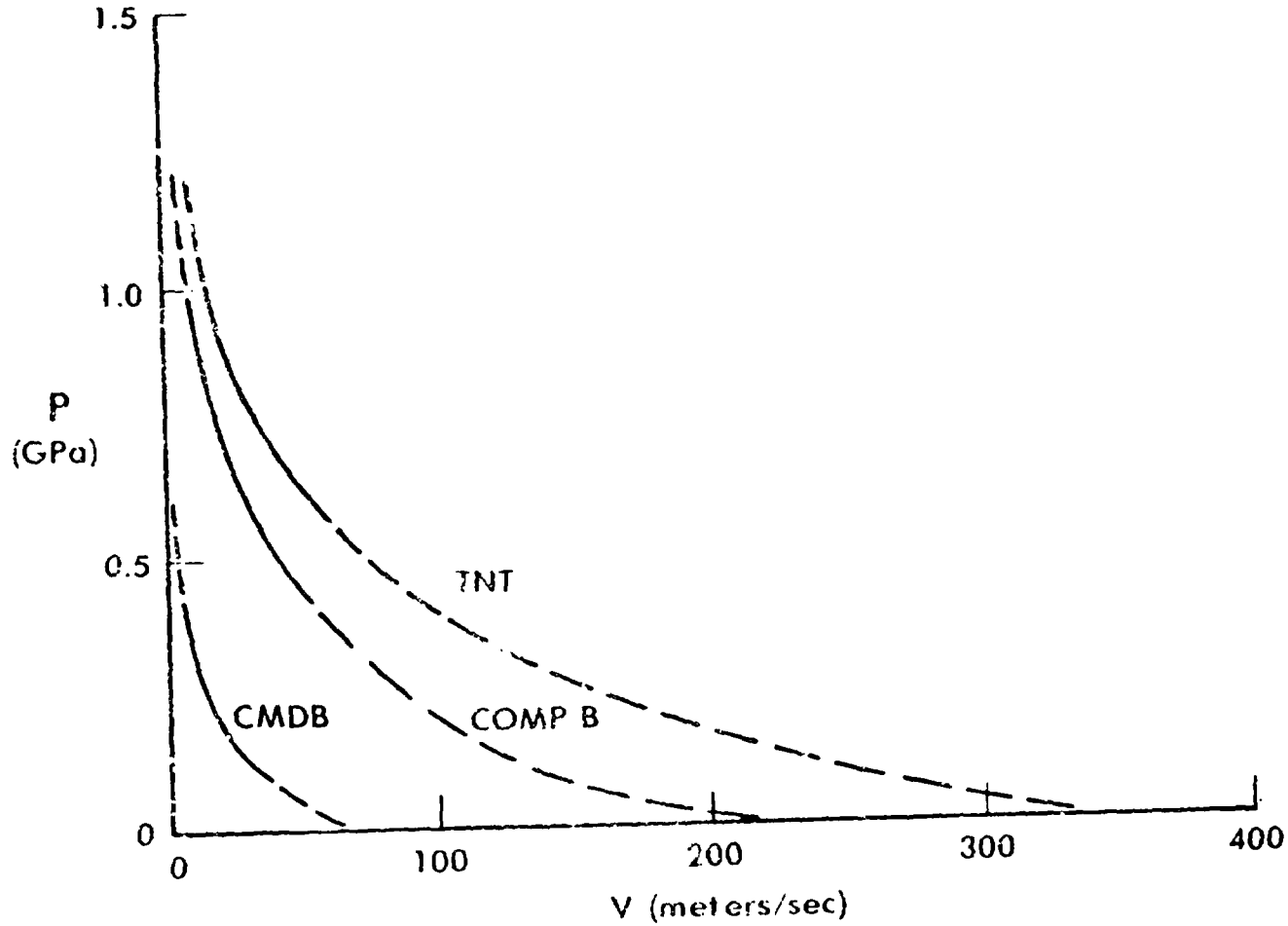

Figure 17. Extrapolation of the curve $e^{\frac{P}{P_R} V_1^2}$ = constant for TNT, Comp B and CMDB.

From the form of Equation 13, it can be seen that the maximum temperature in the shear band, T_1, increases monotonically with viscosity, pressure, and the velocity gradient across the shear band and is inversely proportional to the thermal conductivity of the explosive. By substituting values for μ_R, λ_o, T_R, P_R, and P, V_1 along the TNT isotherm, Equation 13 can be rewritten

$$\frac{T_1 - T_0}{e^{\frac{7760}{T_1+T_0}}} = \frac{\left(1.39\times10^{-2}\right)e^{\frac{0.800}{0.165}}(30)^2}{4\,(0.262)e^{\frac{3880}{358}}}$$

$$\frac{T_1 - T_0}{e^{\frac{7760}{T_1+T_0}}} = 2.99\times10^{-2} \qquad (14)$$

By iteration of Equation 14, we obtain $T_1 = 560^{\circ}K = 287^{\circ}C$ for the maximum shear band temperature. This temperature seems to be too low to explain reaction that occurs in about one millisecond in our experiments. The adiabatic thermal explosion formula[11] requires a temperature of $490^{\circ}C$ for TNT to react in one millisecond. The approximate nature of our calculations and the uncertainty of the estimated values of the coefficients of viscosity and thermal conductivity may explain the low value of T_1.

6. DISCUSSION

The data which we have presented indicate that ignition sensitivity increases from TNT to Comp B to CMDB propellant. We believe that ignition occurs as a result of viscous heating concentrated in a small volume of explosive as it shears under pressure. Both pressure and temperature have a large effect on viscosity. This is illustrated in Figure 18 where the logarithm of $\bar{\mu}$ (average viscosity) is plotted against pressure for several values of average temperature. The average viscosity was calculated from Equation 3. It can be seen that viscosity increases with pressure and decreases as the temperature increases. In our shear experiments, the explosive starts to heat as it resists the shearing force. Some region of the shear band reaches a maximum temperature due to non-uniform heating across the shear band and thermal loss at the boundary. Since the explosive is thermally softened in the region of maximum temperature, the velocity gradient increases in this region. The thermal energy deposition

rate per unit volume, Equation 2, is proportional to the square of the velocity gradient. If this rate is high enough, the explosive will ignite. At the boundary between ignition and non-ignition, the maximum temperature will be limited by thermal conduction across the shear band. Using this physical hypothesis, we have deliberately fit our data to a viscous heating model as indicated by Equation 7. This equation describes an isotherm at the boundary between ignition and non-ignition. For a given explosive, we have used Equation 8 to fit the experimental data

Although our data show a large amount of scatter, the curve,

$e^{\frac{P}{P_R}} V_1^2 = \text{constant}$ appears to give a satisfactory fit. The data for TNT on TNT and TNT on steel were fit using the same curve. This suggests that the thermal conductivity of the steel boundary which, is 2 orders of magnitude higher than TNT, played no significant ignition role in our tests. The same was true for Comp B on Comp B and Comp B on steel data. One reason for this may be that the relatively long rise time, 500 microseconds, of our experiment and thermal transport at the explosive-steel boundary allowed the region of maximum temperature to migrate into the explosive giving results compatible with explosive on explosive shear.

We are aware of the excellent results of Randolph et al[10] on the oblique impact ignition of PBX 9404 which show that the thermal conductivity of the target has a large effect on ignition sensitivity. In their tests, a hemispherical billet of PBX 9404 was impacted against inclined targets of widely varying thermal conductivity. Low thermal conductivity targets sensitized ignition whereas high thermal conductivity targets desensitized ignition. Although our activator tests and the oblique impact tests are basically explosive shear tests, we think some reasons for the different results may be due to the dynamic history of each test as follows:

Activator tests achieve peak pressure and shear velocity gradient in about 500 microseconds. By this time, due to thermal conductivity, the maximum temperature may have migrated to the interior of the shearing explosive and be insensitive to thermal transport at the explosive-steel boundary.

In the oblique impact test, the maximum shear velocity gradient and heat generation occur at the beginning. This implies that heat transport can have a large effect on the peak temperature.

In the oblique impact test, the motion of the impacting billet towards the target interface tends to keep the high temperature region close to the interface.

PBX 9404 is a brittle explosive with a small amount of binder. This implies a narrow shear zone which can be affected by heat transport.

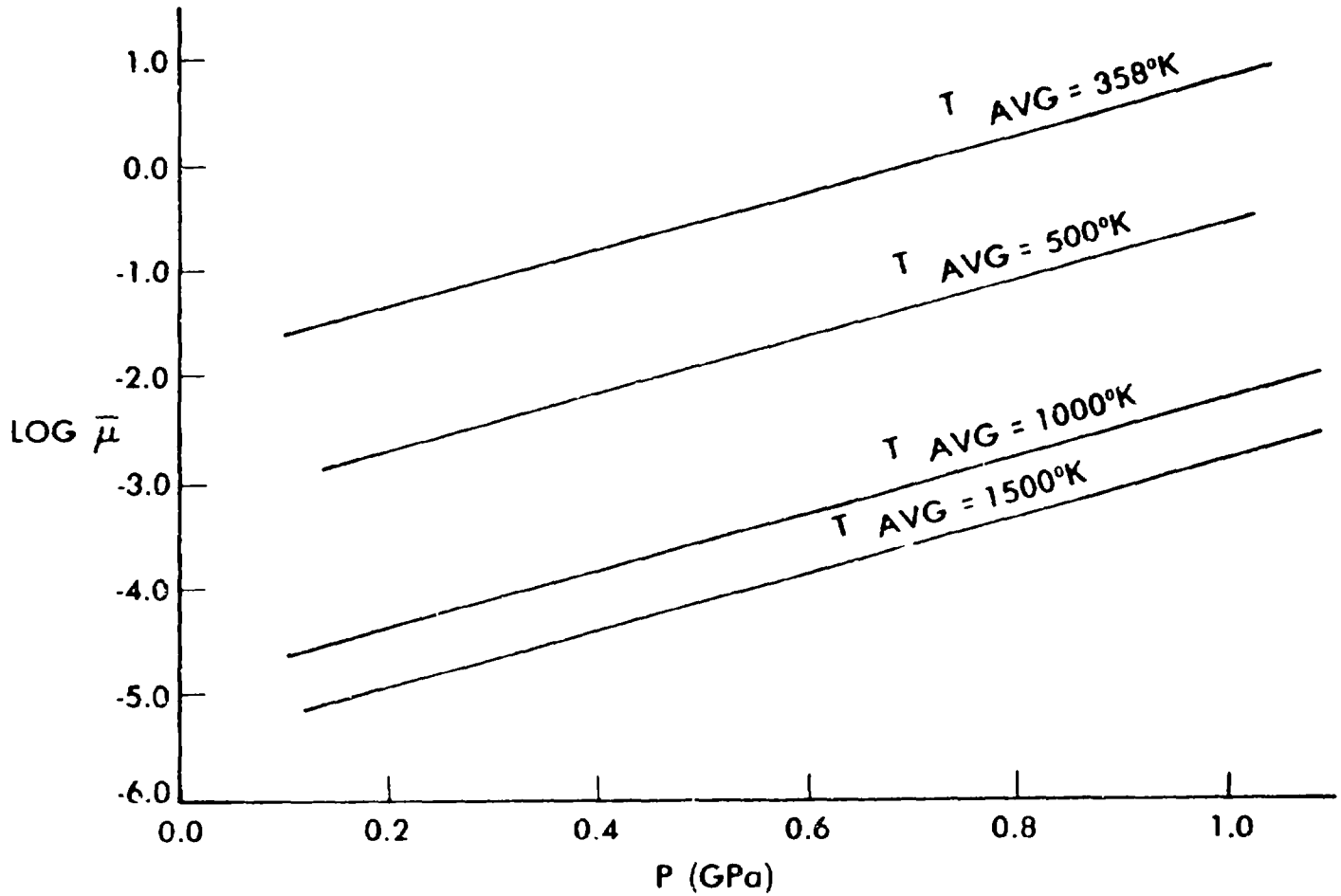

Figure 18. Both pressure and temperature have a large effect on viscosity as illustrated here where the logarithm of the average viscosity is plotted vs pressure for a range of temperature. The average viscosity was calculated using eq. 3.

There was evidence of localized heating in many of the unreacted test samples. A visual examination showed a narrow ring of plastically deformed explosive at the boundaries of both the sheared plug and the remaining annulus. This ring was darker and more uniform than the original explosive. Figure 19 is a 100 times magnification of the inner circumference of the annulus remaining after a 12.7mm diameter plug had been sheared from a 19.1mm diameter Comp B sample at a pressure of 0.1 GPa and a velocity of 30 m/sec. The width of the plastically deformed ring is about 100 microns. The sheared plug also showed a similar ring of about 100 microns width. At higher pressure and sliding velocity, the explosive at the shear boundary appeared to have melted and resolidified. Sometimes a thin layer of explosive adhered to the surface of the buffer plug. CMDB propellant indicated similar phenomena.

Under marginal ignition conditions, Comp B usually burned completely. TNT sometimes burned completely, producing a large quantity of soot or it started to burn and died out leaving a central plug and annulus with charred shear boundary surfaces. CMDB propellant sometimes burned completely or it started to burn and then died out in a manner similar to TNT. In one recovered sample, the burn appeared to have originated at the shear boundary and propagated radially for a distance of 1.5mm into both the sheared plug and the annulus before dying out. In several of the reacted CMDB propellant shots, the residue consisted of a fragile skeletal structure of small spheres of aluminum. We assume this structure was formed by the melting and resolidification of the fine aluminum particles contained in the propellant.

The physical evidence of the recovered samples indicates that a narrow region of explosive around the shear boundary heats up and ignition starts in this region. The appearance of the heated region implies a viscous heating process and we have attempted to interpret our data in terms of such a process.

Our experimental data for CMDB propellant indicated that it was very sensitive, as shown in Figure 15. CMDB is a composite, modified, double base (nitrocellulose, nitroglycerine) propellant containing aluminum. We suspect that the high viscosity of nitrocellulose may be a significant contributor to shear ignition sensitivity.

A possible source of extraneous ignition in these experiments may be the high temperatures caused by metal on metal friction such as might occur between the piston and the confinement cylinder (Figure 1) or between the steel sleeve and its confinement cylinder (Figure 2). Another source of extraneous ignition may be explosive heating due to the large shear velocity gradient when a thin layer of explosive flows between these boundary discontinuities. We tried to prevent or minimize these effects by the use of buffer plugs next to the explosive and strong end plates on the

confinement cylinder. In one test of TNT sliding against steel, we did not use any buffer plugs and the pressurized explosive flowed between the steel pistons and the confinement cylinder bore, depositing a layer of unreacted explosive on the ends of the confinement cylinder. The pressure on the TNT sample was 0.5 GPa and the width of the flow channel was estimated to be less than 25 microns. In this case, the close proximity of the surrounding steel surfaces may have had a large cooling effect on the thin layer of explosive flowing between them.

In some of our high pressure shots for explosive on explosive shear using the experimental arrangement of Figure 2, explosive flowed into the joint between the steel sleeves. We speculate that the end plates flexed due to the force of the pressurized explosive acting on the internal surfaces of the steel sleeves. This would create a gap between the steel sleeves allowing a thin layer to flow radially into the gap. In order to prevent this radial flow, we have started using the experimental arrangement depicted in Figure 20. We are presently evaluating the effectiveness of this design.

7. CONCLUSIONS

The data of our combined pressure-shear ignition experiments indicate an increasing sensitivity from TNT to Comp B to CMDB propellant. We have assumed viscoplastic heating within the shear zone and calculated (using many approximations) an energy deposition rate per unit volume. This calculation was interpreted in terms of an isotherm that defines the boundary between ignition and non-ignition.

We did not see any difference in ignition sensitivity between explosive slid on explosive and explosive slid on steel in these experiments. However, the large spread in our data may have precluded such an observation. We speculate that the high sensitivity of CMDB propellant to combined pressure-shear ignition may be due to its highly viscous nitrocellulose component.

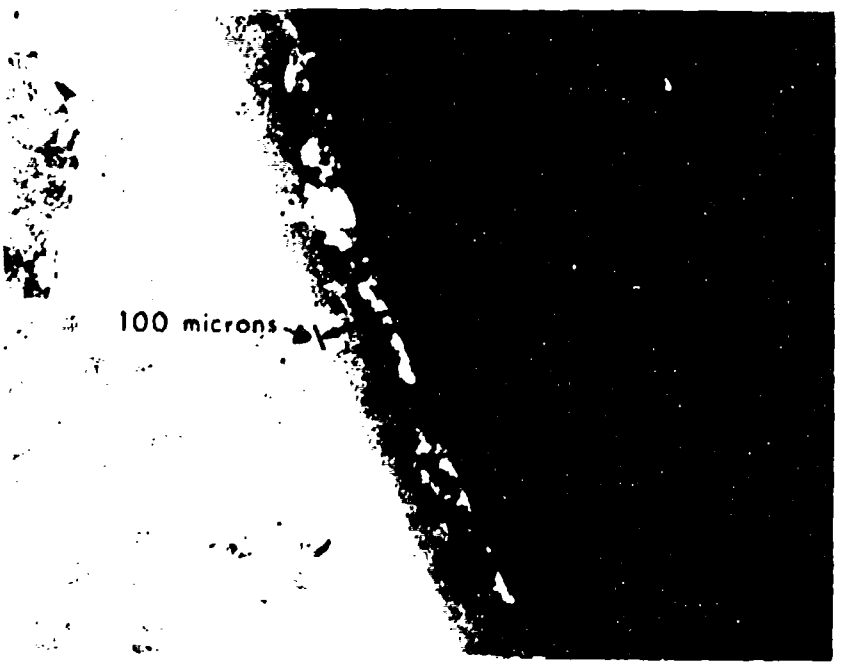

Figure 19. Comp B on Comp B shear, no reaction. This is a 100x magnification of the inner circumference of the annulus remaining after a plug had been sheared out at a pressure of 0.1 GPa and a shear velocity of 25m/sec. The width of the plastically deformed region is abou 100 microns.

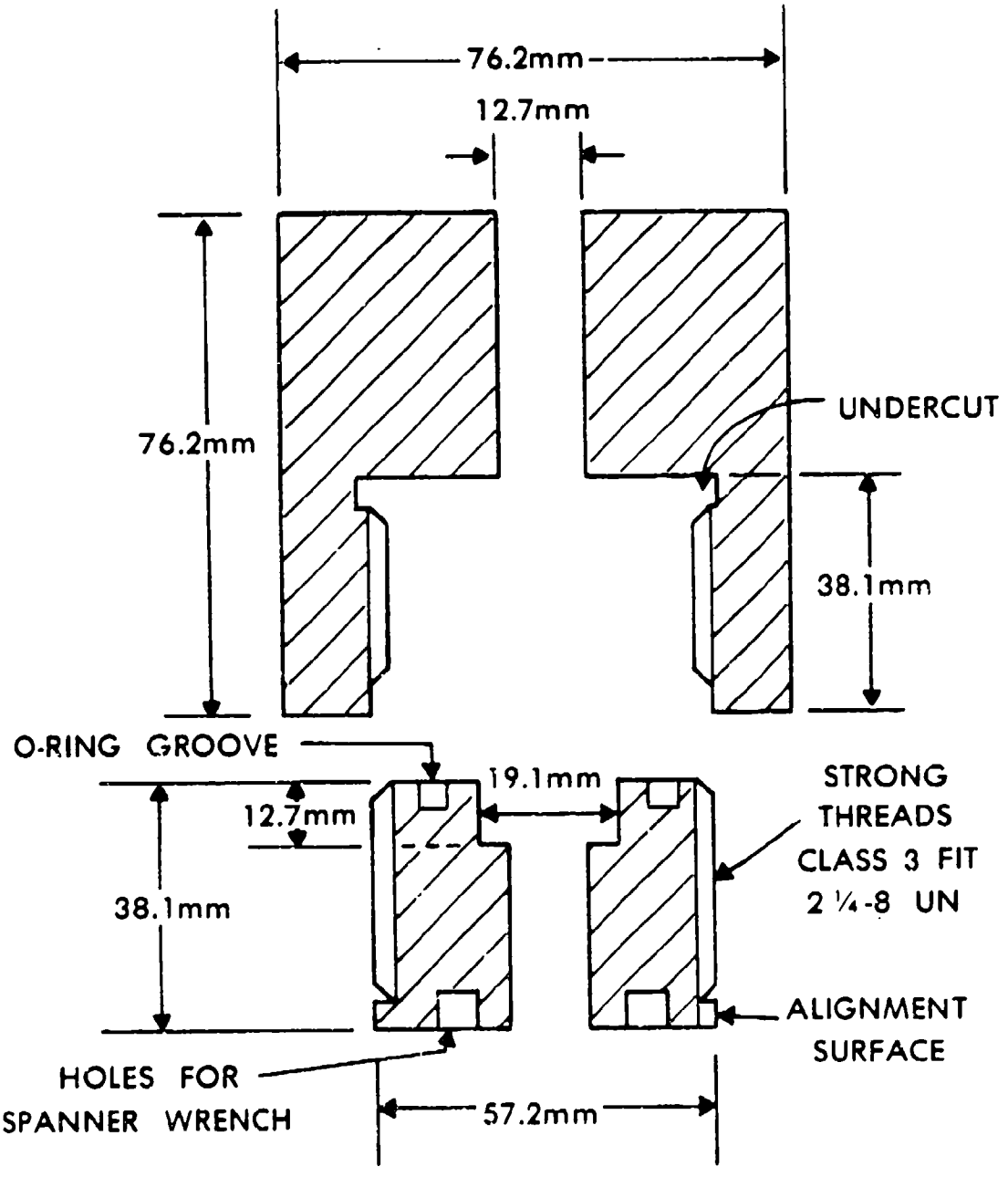

Figure 20. Experimental design to prevent radial flow during shear by providing stronger confinement around the explosive sample.

References

1. T.R. Gibbs and Alphonse Popolato, eds., LASL Explosive Property Data, University of California Press, Los Angeles, CA, 1980.

2. M. Kipp, "Modeling Granular Explosive Detonations With Shear Band Concepts," Eighth Symposium (International) on Detonation, Preprints, Volume 2, July 1985.

3. S.N. Heavens and J.E. Field, "The Ignition of a Thin Layer of Explosive by Impact," Proceedings of the Royal Society of London, A338, 77-93, 1974.

4. R. Winter and J. Field, "The Role of Localized Plastic Flow in the Impact Initiation of Explosives," Proceedings of the Royal Society of London, A343, 1975.

5. C.S. Coffey, "Hot Spot Production by Moving Dislocations in a Rapidly Deforming Crystalline Explosive," Eighth Symposium (International) on Detonation, Preprints, Volume 2, July 1985.

6. B.C. Taylor and L.H. Ervin, "Mode of Ignition in the Picatinny Arsenal Activator (Artillery Setback Simulator)," Special Publication ARLCD-SP-77004, Proceedings of the Conference on the Standardization of Safety and Performance Tests for Energetic Materials - Volume I, ARRADCOM, Dover, NJ, September 1977.

7. R.B. Frey, "The Initiation of Explosive Charges by Rapid Shear," Seventh Symposium (International) on Detonation, Naval Surface Weapons Center, NSWC MP 82-334, 1981.

8. Robert B. Frey, "Cavity Collapse in Energetic Materials," BRL-TR-2748, July 1986.

9. R.N. Rogers, "Thermochemistry of Explosives," Thermochemica Acta, 11, 1975.

10. Alan D. Randolph, L.E. Hatler, and A. Popolato, "Rapid Heating to Ignition of High Explosives, I. Friction Heating," Ind. Eng. Chem., Fundamentals, Volume 15, No. 1, 1976.

11. Engineering Design Handbook-Principles of Explosive Behavior, pg 10-10, AMC Pamphlet No. 706-180, 1972.

APPENDIX A

Derivation of Equation

Referring to Figure 7, it can be seen $\Delta V = \frac{eR}{2R} - \frac{eR}{2R+\Delta R}$

since $\alpha = \frac{\frac{\Delta R}{R}}{P}$

or $\Delta R = \alpha PR$ we can write

$$\Delta V = \frac{eR}{2R} - \frac{eR}{2R+\alpha PR}$$

$$\Delta V = \frac{e}{2} - \frac{e}{2+\alpha P}$$

$$\Delta V = \frac{\alpha eP}{2(2+\alpha P)}$$

$$4\Delta V + 2\alpha P\Delta V = \alpha eP$$

$$P = \frac{4\Delta V}{\alpha e - 2\alpha\Delta V} \approx \frac{4\Delta V}{\alpha e} \cdot \text{for } e \gg \Delta V$$

e = Bridge Input Voltage (Volts)
R = Gage Resistance (ohms)
ΔR = Change in Gage Resistance (ohms)
ΔV = Bridge Output Signal (Volts)
P = Pressure (GPa)
α = Pressure Coefficient of Resistance for Manganin = .023 $\frac{\text{ohm}}{\text{ohm-GPa}}$

SYMBOLS

E .....Experimentally Determined Constant = 3880°K

P .....Pressure in Shear Band, GPa

P_R .....Experimentally Determined Constant = 0.165 GPa

T_O .....Constant Initial Temperature = 293°K

T_R .....Reference Temperature for Calculating Viscosity = 358°K

T .....Temperature in Shear Band, °K

T_1 .....Peak Temperature in Shear Band, °K

T_{AVG} .....Average Temperature in Shear Band, °K

V .....Shear Velocity Across Shear Band, m/sec

V_1 .....Maximum Shear Velocity Across Shear Band, m/sec

V_{AVG} .....Average Shear Velocity Across Shear Band, m/sec

Z .....Width of Shear Band, m

$\frac{dV}{dz}$ .....Shear Velocity Gradient, $\frac{1}{sec}$

$\frac{\Delta V}{\Delta Z}$ .....Average Shear Velocity Gradient, $\frac{1}{sec}$

$\frac{\Delta T}{\Delta Z}$ .....Average Temperature Gradient Across Shear Band, $\frac{°K}{m}$

e .....Base of the Natural Log = 2.71828

μ .....Viscosity, $\frac{kg}{m\text{-}sec}$

$\bar{\mu}$ .....Average Viscosity, $\frac{kg}{m\text{-}sec}$

μ_R .....Viscosity of TNT at 358°K = 1.39×10^{-2} $\frac{kg}{m\text{-}sec}$

λ_0 .....Thermal Conductivity of TNT at 293°K = .262 $\frac{joule}{m\text{-}°K\text{-}sec}$

DISTRIBUTION LIST

No. of Cys	Organization
12	Administrator Defense Technical Info Center ATTN: DTIC-FDAC Cameron Station, Bldg 5 Alexandria, VA 22304-6145
1	HQDA (DAMA-ART-M) WASH DC 20310
1	Chairman DOD Explosives Safety Board ATTN: COL Powell, Rm 856-C Hoffman Bldg 1 2461 Eisenhower Avenue Alexandria, VA 22331
1	Commander USA Materiel Command ATTN: AMCDRA-ST 5001 Eisenhower Avenue Alexandria, VA 22333-0001
3	Commander USA Armament Research Development & Engineering Center ATTN: SMCAR-MSI SMCAR-TDC SMCAR-LCE (Dr. Slagg) Picatinny Arsenal, NJ 07806-5000
1	Commander USA Armament, Munitions & Chemical Command ATTN: AMSMC-IMP-L Rock Island, IL 61299-7300
1	Director Benet Weapons Laboratory ATTN: SMCAR-CCB-TL Watervliet, NY 12189-4050
1	Commander USA Aviation Systems Command ATTN: AMSAV-ES 4300 Goodfellow Boulevard St. Louis, MO 63120-1798
1	Director USA Aviation Research & Technology Activity Ames Research Center Moffett Field, CA 94035-1099
2	Commander USA Communications Electronics Command ATTN: AMSEL-ED AMSEL-IM-L (Reports Section) B2700 Fort Monmouth, NJ 07703
1	Commander USA Missile Command ATTN: AMSME-RK (Dr. Rhoades) Redstone Arsenal, AL 35898-5500
1	Commander MICOM Research, Development and Engineering Center ATTN: AMSMI-RD Redstone Arsenal, AL 35898
1	Director Missile & Space Intelligence Center ATTN: AIAMS-YDL Redstone Arsenal, AL 35898-5500
1	Commander USA Tank Automotive Command ATTN: AMSTA-TSL Warren, MI 48397-5000
1	Director USA TRADOC Analysis Center ATTN: ATOR-TSL White Sands Missile Range, NM 88002-5502
1	Commandant USA Infantry School ATTN: ATSH-CD-CS-OR Fort Benning, GA 31905-5400

DISTRIBUTION LIST

No. of Cys	Organization
1	Commander USA Development & Employment Agency ATTN: MODE-ORO Fort Lewis, WA 98433-5000
1	Commander USA Research Office ATTN: Chemistry Division P.O. Box 12211 Research Triangle Park, NC 27709-2211
2	Office of Naval Research ATTN: Code 23 (Dr. Faulstick) 800 N. Quincy Street Arlington, VA 22217
1	Commander Naval Sea Systems Command ATTN: SEA 06I (Dr. R. Bowen) Washington, DC 20362
1	Commander Naval Explosive Ordnance Disposal Technology Center ATTN: Code 604 (Tech Library) Indian Head, MD 20640
1	Commander Naval Research Lab ATTN: Code 6100 Washington, DC 20375
1	Commander Naval Surface Weapons Center ATTN: Code G13 Dahlgren, VA 22448-5000
6	Commander Naval Surface Weapons Center ATTN: R10 (S.J. Jacobs) R10B (Mr. M. Stosz) R10C (Mr. L. Roslund) Code X211 (Library) R12 (Short) R13 (Bernecker/Forbes) Silver Spring, MD 20902-5000
4	Commander Naval Weapons Center ATTN: Code 326 (Dr. L. Smith) Code 385 (Dr. R. Atkins) Code 388 (Dr. R. Reed) Code 3891 (Dr. K. Graham) China Lake, CA 93555
1	Commander Naval Weapons Station, NEDED ATTN: Code 50 (Dr. Rothstein) Yorktown, VA 23691
1	Commander Fleet Marine Force, Atlantic ATTN: G-4 (NSAP) Norfolk, VA 23511
1	Commander Air Force Rocket Propulsion Laboratory ATTN: Code AFRPL MKPA (Mr. R. Geisler) Edwards AFB, CA 93523
1	AFWL/SUL Kirtland AFB, NM 87117
1	AFATL/DOIL (Tech Info Center) Eglin AFB, FL 32542-5438
1	Commander Ballistic Missile Defense Advanced Technology Center ATTN: Dr. David C. Sayles P.O. Box 1500 Huntsville, AL 35807
1	Director Lawrence Livermore National Laboratory University of California ATTN: Dr. M. Finger P.O. Box 808 Livermore, CA 94550

DISTRIBUTION LIST

No. of Cys	Organization
1	Director Los Alamos National Laboratory ATTN: Mr. J. Ramsey P.O. Box 1663 Los Alamos, NM 87545
1	Sandia National Laboratories ATTN: Dr. E. Mitchell, Supv, Division 2513 P.O. Box 5800 Albuquerque, NM 87185
10	Central Intelligence Agency OIR/DB/Standard GE47 HQ Washington, DC 20505
1	Southwest Research Institute ATTN: M. Cowperthwaite 6220 Culebra Road Postal Draweer 28510 San Antonio, TX 78284
1	New Mexico Institute of Mining and Technology Campus Station ATTN: TERA/T. Joyner Socorro, NM 87801

Aberdeen Proving Ground

Cdr, CRDEC, ATTN:	SMCCR-RSP-A
	SMCCR-MU
	SMCCR-SPS-IL
Cdr, TECOM, ATTN:	AMSTE-SI-F
Dir, USAMSAA, ATTN:	AMXSY-D
	AMXSY-MP (Cohen)

USER EVALUATION SHEET/CHANGE OF ADDRESS

This Laboratory undertakes a continuing effort to improve the quality of the reports it publishes. Your comments/answers to the items/questions below will aid us in our efforts.

1. BRL Report Number _____ Date of Report _____

2. Date Report Received _____

3. Does this report satisfy a need? (Comment on purpose, related project, or other area of interest for which the report will be used.) _____

4. How specifically, is the report being used? (Information source, design data, procedure, source of ideas, etc.) _____

5. Has the information in this report led to any quantitative savings as far as man-hours or dollars saved, operating costs avoided or efficiencies achieved, etc? If so, please elaborate. _____

6. General Comments. What do you think should be changed to improve future reports? (Indicate changes to organization, technical content, format, etc.)

_____

_____

_____

CURRENT ADDRESS

_____
Name

_____
Organization

_____
Address

_____
City, State, Zip

7. If indicating a Change of Address or Address Correction, please provide the New or Correct Address in Block 6 above and the Old or Incorrect address below.

OLD ADDRESS

_____
Name

_____
Organization

_____
Address

_____
City, State, Zip

(Remove this sheet, fold as indicated, staple or tape closed, and mail.)

FOLD HERE

Director
U.S. Army Ballistic Research Laboratory
ATTN: SLCBR-DD-T
Aberdeen Proving Ground, MD 21005-5066

NO POSTAGE
NECESSARY
IF MAILED
IN THE
UNITED STATES

OFFICIAL BUSINESS
PENALTY FOR PRIVATE USE, $300

BUSINESS REPLY MAIL
FIRST CLASS PERMIT NO 12062 WASHINGTON, DC
POSTAGE WILL BE PAID BY DEPARTMENT OF THE ARMY

Director
U.S. Army Ballistic Research Laboratory
ATTN: SLCBR-DD-T
Aberdeen Proving Ground, MD 21005-9989

FOLD HERE